Mathematical Modelling and Numerical Analysis Will be set by the publisher
Modélisation Mathématique et Analyse Numérique

ON THE EFFECT OF TEMPERATURE AND VELOCITY RELAXATION IN TWO-PHASE FLOW MODELS

Pedro José Martínez Ferrer[1, 2], Tore Flåtten[3, 4] and Svend Tollak Munkejord[3, 5]

Abstract. We study a two-phase pipe flow model with relaxation terms in the momentum and energy equations, driving the model towards dynamic and thermal equilibrium. These equilibrium states are characterized by the velocities and temperatures being equal in each phase. For each of these relaxation processes, we consider the limits of zero and infinite relaxation times. By expanding on previously established results, we derive a formulation of the mixture sound velocity for the thermally relaxed model. This allows us to directly prove a subcharacteristic condition; each level of equilibrium assumption imposed reduces the propagation velocity of pressure waves. Furthermore, we show that each relaxation procedure reduces the mixture sound velocity with a factor that is independent of whether the other relaxation procedure has already been performed.

Numerical simulations indicate that thermal relaxation in the two-fluid model has negligible impact on mass transport dynamics. However, the velocity difference of sonic propagation in the thermally relaxed and unrelaxed two-fluid models may significantly affect practical simulations.

1991 Mathematics Subject Classification. 76T10, 65M08, 35L60.

23rd May 2011.

1. Introduction

During the past decade, there has been significant interest in the applied mathematics community in the study of *hyperbolic relaxation systems* [21,29,31,42], i.e. systems of hyperbolic partial differential equations with stiff source terms driving the solution towards equilibrium. A major influence in this respect was contributed by Chen, Levermore and Liu [8]. In their paper, some key concepts were generalized and analysed:

- The *subcharacteristic condition*, which relates stiff source terms to the propagation velocities of characteristic waves;
- The *Chapman-Enskog expansion*, which relates stiff source terms to diffusion terms.

Keywords and phrases: two-fluid model, relaxation system, subcharacteristic condition

[1] ENSMA, Teleport 2 - 1, Avenue Clement Ader, 86961 Futuroscope Chasseneuil Cedex, France. e-mail: pedro.martinezferrer@ensma.fr

[2] ETSIA, Plaza de Cardenal Cisneros, 3, 28040 Madrid, Spain.

[3] SINTEF Energy Research, P.O. Box 4761 Sluppen, NO-7465 Trondheim, Norway.

[4] e-mail: Tore.Flatten@sintef.no

[5] Corresponding author. e-mail: stm@pvv.org

In the general form presented by Natalini [29], a hyperbolic relaxation problem in the unknown M-vector $\boldsymbol{U}$ can be written as follows:

$$\frac{\partial \boldsymbol{U}}{\partial t} + \boldsymbol{A}(\boldsymbol{U})\frac{\partial \boldsymbol{U}}{\partial x} = \frac{1}{\varepsilon}\boldsymbol{Q}(\boldsymbol{U}), \tag{1}$$

where $\boldsymbol{Q}(\boldsymbol{U})$ is the source term driving the system towards equilibrium, $\boldsymbol{A}$ is diagonalizable with real eigenvalues, and ε is a characteristic relaxation time. Associated with the system is a constant linear operator $\boldsymbol{P} : \mathbb{R}^M \mapsto \mathbb{R}^N$ satisfying

$$\boldsymbol{P}\boldsymbol{Q}(\boldsymbol{U}) = 0 \quad \forall \boldsymbol{U}, \tag{2}$$

where $N < M$. Multiplying (1) by $\boldsymbol{P}$ on the left, we obtain a system of N homogeneous equations

$$\frac{\partial}{\partial t}\left(\boldsymbol{P}\boldsymbol{U}\right) + \boldsymbol{P}\boldsymbol{A}(\boldsymbol{U})\frac{\partial \boldsymbol{U}}{\partial x} = 0. \tag{3}$$

The system (3) may be closed by introducing the *Maxwellian operator* $\mathcal{M} : \Omega \subseteq \mathbb{R}^N \mapsto \mathbb{R}^M$ which satisfies

$$\boldsymbol{Q}\left(\mathcal{M}(\boldsymbol{V})\right) = 0, \tag{4}$$

$$\boldsymbol{P}\mathcal{M}(\boldsymbol{V}) = \boldsymbol{V} \tag{5}$$

for all $\boldsymbol{V} \in \Omega$. In the limit $\varepsilon \to 0$, we expect solutions to the *relaxation system* (1) to approach the equilibrium states $\mathcal{M}(\boldsymbol{V})$, where $\boldsymbol{V}$ are the solutions to the *relaxed system*

$$\frac{\partial \boldsymbol{V}}{\partial t} + \boldsymbol{P}\boldsymbol{A}\left(\mathcal{M}(\boldsymbol{V})\right)\frac{\partial \mathcal{M}(\boldsymbol{V})}{\partial x} = 0. \tag{6}$$

Necessary for linear stability of the relaxation process is the *subcharacteristic condition*, a concept introduced by Liu [23]. A formal, general definition was provided by Chen *et al.* [8]:

Definition 1. *Let the M eigenvalues of the relaxation system* (1) *be given by*

$$\lambda_1 \leq \ldots \leq \lambda_k \leq \lambda_{k+1} \leq \ldots \leq \lambda_M \tag{7}$$

and the N eigenvalues of the relaxed system (4)–(6) *be given by*

$$\tilde{\lambda}_1 \leq \ldots \leq \tilde{\lambda}_j \leq \tilde{\lambda}_{j+1} \leq \ldots \leq \tilde{\lambda}_N. \tag{8}$$

Herein, the relaxation system (1) *is applied to a local equilibrium state $\boldsymbol{U} = \mathcal{M}(\boldsymbol{V})$ such that*

$$\lambda_k = \lambda_k(\mathcal{M}(\boldsymbol{V})), \qquad \tilde{\lambda}_j = \tilde{\lambda}_j(\boldsymbol{V}). \tag{9}$$

Now let the $\tilde{\lambda}_j$ be interlaced *with λ_k in the following sense: Each $\tilde{\lambda}_j$ lies in the closed interval $[\lambda_j, \lambda_{j+M-N}]$ for all $\boldsymbol{V} \in \Omega$. Then the relaxed system* (6) *is said to satisfy the* **subcharacteristic condition** *with respect to* (1).

As pointed out by Natalini [29], this can be interpreted as a causality principle. Source terms act only locally, and can therefore not increase the characteristic speeds of information; this should hold also in the stiff limit $\varepsilon \to 0$. In the present paper, we prove the subcharacteristic condition (in a weak sense made precise in Section 4) for the relaxation processes we are interested in.

For two-phase flows, a general relaxation model was proposed by Baer and Nunziato [2]. Renewed interest in this model was sparked by the works of Abgrall and Saurel [1, 34]. Several authors [3, 4, 11, 13] have used relaxation systems to construct numerical schemes for various two-phase flow models, based on ideas originally suggested by Jin and Xin [20].

More analytical works have also been performed; Murrone and Guillard [28] studied the five-equation model that arises from relaxing the pressure and velocities in the Baer-Nunziato model. This model was also considered

by Saurel *et al.* [35], who included the effect of phase transitions. Zein *et al.* [46] considered the Baer-Nunziato model under velocity equilibrium, including heat and mass transfer terms.

By performing only the pressure relaxation in the Baer-Nunziato model, we recover a six-equation model commonly denoted as the *two-fluid* model [36], consisting of balance equations for mass, momentum and total energy for each phase. Such a model has formed the basis for several computer codes used by the nuclear power industry [6, 39].

If we assume that the phases are close to being in thermal equilibrium, we may simplify this model by taking the limit of zero relaxation time in the heat transfer terms; we then obtain a five-equation model containing a *mixture* energy equation, closed by the assumption of equal temperatures. This model has been widely used by the petroleum industry, forming the basis for the commercially successful OLGA code [5].

This paper is motivated by the observation that this five-equation, two-velocity model has been given little focus in the scientific literature. The main purpose of this paper is to investigate through mathematical analysis and numerical simulations how the thermal equilibrium assumption affects the behaviour of the model.

Our paper is organized as follows: In Section 2, we detail the models we will be working with. In Section 2.1, we restate the formulation of the six-equation two-fluid model presented in [27]. Here a mathematical transformation allows us to express the model without non-conservative time derivatives in the energy equations. In Section 2.2, we assume thermal equilibrium and arrive at the model which will be the main focus of this paper.

In Section 2.3, we consider the stiff limit of the velocity relaxation procedure in the model of Section 2.1, obtaining an original derivation of the five-equation model studied by Murrone and Guillard [28]. In Section 2.4, we present the full equilibrium model.

In Section 3, we present some previously established expressions for the wave velocities of our models. We then derive a quasilinear formulation of the five-equation, two-velocity model and derive analytical wave velocities for this model in equilibrium. In Section 4, we derive some simple relationships between the sound velocities of the reduced models, and show that a subcharacteristic condition holds.

In Section 5, we present a simple approximate Riemann solver for the five-equation two-fluid model. This solver is used in Section 6 to compare the five-equation model to the six-equation model. In Section 7, we summarize our results.

2. The Models

The starting point for our investigations is the following basic pipe-flow model.

- Mass conservation:

$$\frac{\partial}{\partial t}\left(\rho_{\mathrm{g}}\alpha_{\mathrm{g}}\right)+\frac{\partial}{\partial x}\left(\rho_{\mathrm{g}}\alpha_{\mathrm{g}}v_{\mathrm{g}}\right)=0, \tag{10}$$

$$\frac{\partial}{\partial t}\left(\rho_{\ell}\alpha_{\ell}\right)+\frac{\partial}{\partial x}\left(\rho_{\ell}\alpha_{\ell}v_{\ell}\right)=0. \tag{11}$$

$$\tag{12}$$

- Momentum balance:

$$\frac{\partial}{\partial t}\left(\rho_{\mathrm{g}}\alpha_{\mathrm{g}}v_{\mathrm{g}}\right)+\frac{\partial}{\partial x}\left(\rho_{\mathrm{g}}\alpha_{\mathrm{g}}v_{\mathrm{g}}^{2}\right)+\alpha_{\mathrm{g}}\frac{\partial p}{\partial x}+\tau_{\mathrm{i}}=\rho_{\mathrm{g}}\alpha_{\mathrm{g}}g_{x}, \tag{13}$$

$$\frac{\partial}{\partial t}\left(\rho_{\ell}\alpha_{\ell}v_{\ell}\right)+\frac{\partial}{\partial x}\left(\rho_{\ell}\alpha_{\ell}v_{\ell}^{2}\right)+\alpha_{\ell}\frac{\partial p}{\partial x}-\tau_{\mathrm{i}}=\rho_{\ell}\alpha_{\ell}g_{x}. \tag{14}$$

- Energy balance:

$$\frac{\partial E_{\mathrm{g}}}{\partial t}+\frac{\partial}{\partial x}\left(E_{\mathrm{g}}v_{\mathrm{g}}+\alpha_{\mathrm{g}}v_{\mathrm{g}}p\right)+p\frac{\partial \alpha_{\mathrm{g}}}{\partial t}+v_\tau\tau_{\mathrm{i}}=\rho_{\mathrm{g}}\alpha_{\mathrm{g}}v_{\mathrm{g}}g_x+Q, \tag{15}$$

$$\frac{\partial E_{\ell}}{\partial t}+\frac{\partial}{\partial x}\left(E_{\ell}v_{\ell}+\alpha_{\ell}v_{\ell}p\right)+p\frac{\partial \alpha_{\ell}}{\partial t}-v_\tau\tau_{\mathrm{i}}=\rho_{\ell}\alpha_{\ell}v_{\ell}g_x-Q. \tag{16}$$

For each phase $k\in\{\mathrm{g},\ell\}$, we use the following nomenclature:

ρ_k	–	density	$\mathrm{kg/m^3}$,
α_k	–	volume fraction	$\alpha_{\mathrm{g}}+\alpha_\ell=1$,
v_k	–	velocity	m/s,
p	–	common pressure	Pa,
τ_k	–	momentum exchange term	Pa/m,
g_x	–	acceleration of gravity along the x-axis	$\mathrm{m/s^2}$,
e_k	–	specific internal energy i	$\mathrm{m^2/s^2}$,
E_k	–	total energy density	$\mathrm{kg/(m{\cdot}s^2)}$,
v_τ	–	interface velocity	m/s,
Q	–	heat exchange term	$\mathrm{kg/(m{\cdot}s^3)}$,
T_k	–	temperature	K.

This is a rather standard formulation of the model [10, 36], which may be obtained by imposing the pressure equilibrium condition on the full Baer-Nunziato relaxation system [2, 34]. Herein, the total energy density is given by

$$E_k=\rho_k\alpha_k\left(e_k+\frac{1}{2}v_k^2\right). \tag{17}$$

2.1. **The Six-Equation Two-Fluid Model**

For the purposes of this work, we will model the interphasic momentum exchange term as follows:

$$\tau_{\mathrm{i}}=\Delta_{\mathrm{i}}p\frac{\partial\alpha_{\mathrm{g}}}{\partial x}+\mathcal{F}\left(v_{\mathrm{g}}-v_\ell\right), \tag{18}$$

where $\mathcal{F}\geq 0$ is the velocity relaxation coefficient and $\Delta_{\mathrm{i}}p$ is an interface pressure correction term:

$$\Delta_{\mathrm{i}}p=p-p^{\mathrm{i}}, \tag{19}$$

where p^{i} is the pressure at the gas-liquid interface.

Furthermore, the presence of the $\partial_t\alpha$-terms in the energy equations presents an inconvenience for the construction of numerical methods, see for instance [27,30]. We wish to obtain a formulation of the energy equations that involves temporal derivatives only in the variable E_k. Such a formulation was obtained in [27]:

$$\frac{\partial E_{\mathrm{g}}}{\partial t}+\frac{\partial}{\partial x}\left(E_{\mathrm{g}}v_{\mathrm{g}}\right)+\left(\alpha_{\mathrm{g}}v_{\mathrm{g}}-\eta\alpha_{\mathrm{g}}\alpha_\ell\left(v_{\mathrm{g}}-v_\ell\right)\right)\frac{\partial p}{\partial x}+\eta\rho_\ell\alpha_{\mathrm{g}}c_\ell^2\frac{\partial}{\partial x}\left(\alpha_{\mathrm{g}}v_{\mathrm{g}}+\alpha_\ell v_\ell\right)+v_\tau\tau_{\mathrm{i}}=\mathcal{Q}\left(T_\ell-T_{\mathrm{g}}\right)+\rho_{\mathrm{g}}\alpha_{\mathrm{g}}v_{\mathrm{g}}g_x, \tag{20}$$

$$\frac{\partial E_{\ell}}{\partial t}+\frac{\partial}{\partial x}\left(E_{\ell}v_{\ell}\right)+\left(\alpha_\ell v_\ell+\eta\alpha_{\mathrm{g}}\alpha_\ell\left(v_{\mathrm{g}}-v_\ell\right)\right)\frac{\partial p}{\partial x}+\eta\rho_{\mathrm{g}}\alpha_\ell c_{\mathrm{g}}^2\frac{\partial}{\partial x}\left(\alpha_{\mathrm{g}}v_{\mathrm{g}}+\alpha_\ell v_\ell\right)-v_\tau\tau_{\mathrm{i}}=\mathcal{Q}\left(T_{\mathrm{g}}-T_\ell\right)+\rho_\ell\alpha_\ell v_\ell g_x, \tag{21}$$

where η is given by

$$\eta=\frac{p}{\rho_{\mathrm{g}}\alpha_\ell c_{\mathrm{g}}^2+\rho_\ell\alpha_{\mathrm{g}}c_\ell^2} \tag{22}$$

and c_k is the sound velocity

$$c_k^2=\left(\frac{\partial p}{\partial\rho_k}\right)_{s_k},\quad k\in\{\mathrm{g},\ell\}. \tag{23}$$

Furthermore, $\mathcal{Q} \geq 0$ is the temperature relaxation coefficient driving the model towards thermal equilibrium. Following the discussion of [27], we choose the interface velocity

$$v_\tau = \frac{\alpha_\ell \Gamma_\mathrm{g} v_\mathrm{g} + \alpha_\mathrm{g} \Gamma_\ell v_\ell}{\alpha_\ell \Gamma_\mathrm{g} + \alpha_\mathrm{g} \Gamma_\ell} \tag{24}$$

where Γ_k is the Grüneisen coefficient

$$\Gamma_k = \frac{1}{\rho_k} \left(\frac{\partial p}{\partial e_k} \right)_{\rho_k}. \tag{25}$$

As was proved in [27], the equations (20)–(21) are *mathematically equivalent* to (15)–(16), and may be more suitable for the construction of numerical schemes. Note that the source terms are affected by this transformation, so that in general:

$$Q \neq \mathcal{Q}(T_\ell - T_\mathrm{g}). \tag{26}$$

2.1.1. *The Interface Pressure Term*

We now focus on the modelling of the $\Delta_\mathrm{i} p$-term in (18). In the absence of such a correction term, it is a well-known problem [36] that the model (10)–(16) becomes non-hyperbolic with complex eigenvalues. This would generally lead to a lack of existence of stable mathematical solutions to the model, as well as loss of stability of our numerical methods. To avoid such a highly undesirable situation, we follow in the footsteps of much of the existing literature [6, 7, 27, 30] and choose the regularization term introduced by Stuhmiller [37]:

$$\Delta_\mathrm{i} p = \delta \frac{\alpha_\mathrm{g} \alpha_\ell \rho_\mathrm{g} \rho_\ell}{\rho_\mathrm{g} \alpha_\ell + \rho_\ell \alpha_\mathrm{g}} \left(v_\mathrm{g} - v_\ell \right)^2, \tag{27}$$

where the parameter δ is here chosen as

$$\delta = 1.2. \tag{28}$$

Definition 2. *The model given by* (10)–(14), (18)*, as well as* (20)–(28) *will in the following be denoted as the* **six-equation two-fluid model***, or* TF_6 *for short.*

2.2. The Five-Equation Two-Fluid Model

We consider the limit of stiff temperature relaxation in the TF_6-model. That is, we replace (20)–(21) with their sum

$$\frac{\partial}{\partial t} \left(E_\mathrm{g} + E_\ell \right) + \frac{\partial}{\partial x} \left((E_\mathrm{g} + \alpha_\mathrm{g} p) v_\mathrm{g} + (E_\ell + \alpha_\ell p) v_\ell \right) = (\rho_\mathrm{g} \alpha_\mathrm{g} v_\mathrm{g} + \rho_\ell \alpha_\ell v_\ell) g_x, \tag{29}$$

as well as the relation

$$T_\mathrm{g} = T_\ell = T. \tag{30}$$

Definition 3. *The model given by* (10)–(14), (18)*, as well as* (27)–(30) *will in the following be denoted as the* **five-equation two-fluid model***, or* TF_5 *for short.*

We expect solutions of the TF_6 model to converge to the solutions of the TF_5 model in the limit $\mathcal{Q} \to \infty$.

2.3. The Five-Equation Drift-Flux Model

Similarly, we may consider the limit of stiff velocity relaxation in the TF_6-model, i.e. $\mathcal{F} \to \infty$. This limit should correspond to replacing (13)–(14) with their sum, and in addition making the assumption

$$v_\mathrm{g} = v_\ell = v. \tag{31}$$

It now follows from (27) that $\Delta_{\mathrm{i}} p = 0$. It was shown in [15] that this model satisfies the following momentum evolution equations:

$$\frac{\partial}{\partial t}\left(\rho_{\mathrm{g}}\alpha_{\mathrm{g}} v_{\mathrm{g}}\right) + \frac{\partial}{\partial x}\left(\rho_{\mathrm{g}}\alpha_{\mathrm{g}} v_{\mathrm{g}}^2\right) + \frac{\rho_{\mathrm{g}}\alpha_{\mathrm{g}}}{\rho_{\mathrm{g}}\alpha_{\mathrm{g}} + \rho_\ell\alpha_\ell}\frac{\partial p}{\partial x} = \rho_{\mathrm{g}}\alpha_{\mathrm{g}} g_x, \tag{32}$$

$$\frac{\partial}{\partial t}\left(\rho_\ell\alpha_\ell v_\ell\right) + \frac{\partial}{\partial x}\left(\rho_\ell\alpha_\ell v_\ell^2\right) + \frac{\rho_\ell\alpha_\ell}{\rho_{\mathrm{g}}\alpha_{\mathrm{g}} + \rho_\ell\alpha_\ell}\frac{\partial p}{\partial x} = \rho_\ell\alpha_\ell g_x. \tag{33}$$

By comparison with (13)–(14), we find that the limit must satisfy

$$\lim_{\mathcal{F}\to\infty} \tau_{\mathrm{i}} = \left(\frac{\rho_{\mathrm{g}}\alpha_{\mathrm{g}}}{\rho_{\mathrm{g}}\alpha_{\mathrm{g}} + \rho_\ell\alpha_\ell} - \alpha_{\mathrm{g}}\right)\frac{\partial p}{\partial x} \tag{34}$$

which may be substituted in (20)–(21) to obtain the relaxed energy equations. Then the full model may be written as follows:

- Mass conservation:

$$\frac{\partial}{\partial t}\left(\rho_{\mathrm{g}}\alpha_{\mathrm{g}}\right) + \frac{\partial}{\partial x}\left(\rho_{\mathrm{g}}\alpha_{\mathrm{g}} v\right) = 0, \tag{35}$$

$$\frac{\partial}{\partial t}\left(\rho_\ell\alpha_\ell\right) + \frac{\partial}{\partial x}\left(\rho_\ell\alpha_\ell v\right) = 0. \tag{36}$$

- Momentum conservation:

$$\frac{\partial}{\partial t}\left((\rho_{\mathrm{g}}\alpha_{\mathrm{g}} + \rho_\ell\alpha_\ell)v\right) + \frac{\partial}{\partial x}\left((\rho_{\mathrm{g}}\alpha_{\mathrm{g}} + \rho_\ell\alpha_\ell)v^2\right) + \frac{\partial p}{\partial x} = (\rho_{\mathrm{g}}\alpha_{\mathrm{g}} + \rho_\ell\alpha_\ell)g_x, \tag{37}$$

- Energy balance:

$$\frac{\partial E_{\mathrm{g}}}{\partial t} + \frac{\partial}{\partial x}\left(E_{\mathrm{g}} v\right) + v\frac{\rho_{\mathrm{g}}\alpha_{\mathrm{g}}}{\rho_{\mathrm{g}}\alpha_{\mathrm{g}} + \rho_\ell\alpha_\ell}\frac{\partial p}{\partial x} + \eta\rho_\ell\alpha_{\mathrm{g}} c_\ell^2\frac{\partial v}{\partial x} = \mathcal{Q}\left(T_\ell - T_{\mathrm{g}}\right) + \rho_{\mathrm{g}}\alpha_{\mathrm{g}} v_{\mathrm{g}} g_x, \tag{38}$$

$$\frac{\partial E_\ell}{\partial t} + \frac{\partial}{\partial x}\left(E_\ell v\right) + v\frac{\rho_\ell\alpha_\ell}{\rho_{\mathrm{g}}\alpha_{\mathrm{g}} + \rho_\ell\alpha_\ell}\frac{\partial p}{\partial x} + \eta\rho_{\mathrm{g}}\alpha_\ell c_{\mathrm{g}}^2\frac{\partial v}{\partial x} = \mathcal{Q}\left(T_{\mathrm{g}} - T_\ell\right) + \rho_\ell\alpha_\ell v_\ell g_x. \tag{39}$$

Definition 4. *The model given by* (31)–(39) *will in the following be denoted as the* **five-equation drift-flux model**, *or* DF_5 *for short.*

We observe that the DF_5 model derived here is equivalent to the two-component version of the model considered in [17]. There, it was also shown that this two-component model, and hence the DF_5 model, is equivalent to models studied in [28, 35].

Remark 1. *The term "drift-flux" is commonly associated with dynamic equilibrium models where $v_{\mathrm{g}} \neq v_\ell$, see for instance [47]. However, in the petroleum industry, one typically separates between "two-fluid" models, where the velocities evolve separately, and "drift-flux" models, where the velocities are coupled through a functional relation [25]. This motivates our choice of terminology. We also remark that there is some reason to expect that the main conclusions of this paper may carry over to the more general case where $v_{\mathrm{g}} \neq v_\ell$, a question that may possibly be further investigated through an asymptotic analysis following for instance the approach of [15, 41].*

2.4. The Four-Equation Drift-Flux Model

To obtain the full equilibrium model, we replace (38)–(39) with their sum

$$\frac{\partial}{\partial t}\left(E_{\mathrm{g}} + E_\ell\right) + \frac{\partial}{\partial x}\left((E_{\mathrm{g}} + E_\ell + p)v\right) = v(\rho_{\mathrm{g}}\alpha_{\mathrm{g}} + \rho_\ell\alpha_\ell)g_x, \tag{40}$$

and impose the thermal equilibrium condition

$$T_{\mathrm{g}} = T_{\ell} = T. \tag{41}$$

Definition 5. *The model given by* (35)–(37)*, as well as* (40)–(41) *will in the following be denoted as the* **four-equation drift-flux model***, or* DF_4 *for short.*

This should correspond to the limit $\mathcal{Q} \to \infty$ in the DF_5 model. Alternatively, the DF_4 model may be obtained as the limit of stiff velocity relaxation in the TF_5 model, i.e. $\mathcal{F} \to \infty$. In this case, (13)–(14) are replaced with their sum, and the relation

$$v = v_{\mathrm{g}} = v_{\ell} \tag{42}$$

is imposed.

As we are interested in studying the limits of zero and infinite relaxation times, we will for the remainder of this paper assume

$$\mathcal{Q} = 0 \tag{43}$$

for the TF_6 and DF_5 models.

3. Wave Velocities

In this section, we present exact analytical expressions for the wave velocities of our models, evaluated at the equilibrium state where

$$T = T_{\mathrm{g}} = T_{\ell}, \tag{44}$$

$$v = v_{\mathrm{g}} = v_{\ell}. \tag{45}$$

From these expressions, we will show in Section 4 that the relaxation processes satisfy a subcharacteristic condition.

In this respect, our main contribution is the analysis for the TF_5 model, which will be presented in Section 3.4. We first briefly review some known results for the other models.

3.1. The Six-Equation Two-Fluid Model

For a general state where $v_{\mathrm{g}} \neq v_{\ell}$, the eigenvalues of this model are the roots of a 6-degree polynomial for which no simple closed forms can in general be found. This model was studied by Toumi [41], who suggested deriving a power series expansion in terms of the variable

$$\xi = \frac{v_{\mathrm{g}} - v_{\ell}}{c_{\mathrm{TF}_6}}, \tag{46}$$

where c_{TF_6} is given by

$$c^2_{\mathrm{TF}_6} = c^2_{\mathrm{g}} c^2_{\ell} \frac{\rho_{\ell}\alpha_{\mathrm{g}} + \rho_{\mathrm{g}}\alpha_{\ell}}{\rho_{\ell}\alpha_{\mathrm{g}} c^2_{\ell} + \rho_{\mathrm{g}}\alpha_{\ell} c^2_{\mathrm{g}}}. \tag{47}$$

To lowest order, i.e. when (45) is satisfied, one obtains the eigenvalues

$$\mathbf{\Lambda}_{\mathrm{TF}_6} = \begin{bmatrix} v - c_{\mathrm{TF}_6} \\ v \\ v \\ v \\ v \\ v + c_{\mathrm{TF}_6} \end{bmatrix}, \tag{48}$$

see [41] for details.

3.2. **The Five-Equation Drift-Flux Model**

This model has been extensively analysed by several authors [17, 28, 35], and the resulting eigenvalues are

$$\mathbf{\Lambda}_{\mathrm{DF}_5} = \begin{bmatrix} v - c_{\mathrm{DF}_5} \\ v \\ v \\ v \\ v + c_{\mathrm{DF}_5} \end{bmatrix}. \tag{49}$$

Herein, c_{DF_5} is a well-known, classic expression sometimes referred to as the "Wood speed of sound" [35], given by

$$c_{\mathrm{DF}_5}^{-2} = (\rho_{\mathrm{g}}\alpha_{\mathrm{g}} + \rho_\ell\alpha_\ell)\left(\frac{\alpha_{\mathrm{g}}}{\rho_{\mathrm{g}}c_{\mathrm{g}}^2} + \frac{\alpha_\ell}{\rho_\ell c_\ell^2}\right). \tag{50}$$

3.3. **The Four-Equation Drift-Flux Model**

The N-component version of this model was the main focus of [17]. For our present case of $N = 2$, the following eigenvalues were found:

$$\mathbf{\Lambda}_{\mathrm{DF}_4} = \begin{bmatrix} v - c_{\mathrm{DF}_4} \\ v \\ v \\ v + c_{\mathrm{DF}_4} \end{bmatrix}, \tag{51}$$

where

$$c_{\mathrm{DF}_4}^{-2} = c_{\mathrm{DF}_5}^{-2} + \frac{\rho_{\mathrm{g}}\alpha_{\mathrm{g}} + \rho_\ell\alpha_\ell}{T}\frac{C_{p,\mathrm{g}}C_{p,\ell}(\zeta_{\mathrm{g}} - \zeta_\ell)^2}{C_{p,\mathrm{g}} + C_{p,\ell}}, \tag{52}$$

where C_p is the extensive heat capacity

$$C_{p,k} = \rho_k\alpha_k c_{p,k}, \qquad c_{p,k} = T\left(\frac{\partial s_k}{\partial T}\right)_p, \tag{53}$$

and ζ_k is the parameter

$$\zeta_k = \left(\frac{\partial T}{\partial p}\right)_{s_k} = -\frac{1}{\rho_k^2}\left(\frac{\partial \rho_k}{\partial s_k}\right)_p. \tag{54}$$

Herein, s_k is the specific entropy.

3.4. **The Five-Equation Two-Fluid Model**

In order to calculate the wave velocities of the TF_5 model, we will present an analytical expression for the Jacobian matrix. This model can be written as follows:

$$\frac{\partial \boldsymbol{U}}{\partial t} + \frac{\partial \boldsymbol{F}(\boldsymbol{U})}{\partial x} + \mathbf{B}(\boldsymbol{U})\frac{\partial \boldsymbol{W}(\boldsymbol{U})}{\partial x} = \boldsymbol{S}(\boldsymbol{U}), \tag{55}$$

with

$$\boldsymbol{U} = \begin{bmatrix} u_1 \\ u_2 \\ u_3 \\ u_4 \\ u_5 \end{bmatrix} = \begin{bmatrix} \rho_{\mathrm{g}}\alpha_{\mathrm{g}} \\ \rho_\ell\alpha_\ell \\ \rho_{\mathrm{g}}\alpha_{\mathrm{g}}v_{\mathrm{g}} \\ \rho_\ell\alpha_\ell v_\ell \\ E \end{bmatrix} = \begin{bmatrix} m_{\mathrm{g}} \\ m_\ell \\ I_{\mathrm{g}} \\ I_\ell \\ E_{\mathrm{g}} + E_\ell \end{bmatrix}, \quad \boldsymbol{F}(\boldsymbol{U}) = \begin{bmatrix} \rho_{\mathrm{g}}\alpha_{\mathrm{g}}v_{\mathrm{g}} \\ \rho_\ell\alpha_\ell v_\ell \\ \rho_{\mathrm{g}}\alpha_{\mathrm{g}}v_{\mathrm{g}}^2 + \alpha_{\mathrm{g}}\Delta_{\mathrm{i}}p \\ \rho_\ell\alpha_\ell v_\ell^2 + \alpha_\ell\Delta_{\mathrm{i}}p \\ E_{\mathrm{g}}v_{\mathrm{g}} + E_\ell v_\ell + p\left(\alpha_{\mathrm{g}}v_{\mathrm{g}} + \alpha_\ell v_\ell\right) \end{bmatrix}, \tag{56}$$

$$\mathbf{B}(\boldsymbol{U}) = \begin{bmatrix} 0 & 0 \\ 0 & 0 \\ \alpha_{\mathrm{g}} & -\alpha_{\mathrm{g}} \\ \alpha_{\ell} & -\alpha_{\ell} \\ 0 & 0 \end{bmatrix}, \quad \boldsymbol{W}(\boldsymbol{U}) = \begin{bmatrix} p \\ \Delta_{\mathrm{i}} p \end{bmatrix}, \quad \boldsymbol{S}(\boldsymbol{U}) = \begin{bmatrix} 0 \\ 0 \\ \rho_{\mathrm{g}} \alpha_{\mathrm{g}} g_x \\ \rho_{\ell} \alpha_{\ell} g_x \\ \left(\rho_{\mathrm{g}} \alpha_{\mathrm{g}} v_{\mathrm{g}} + \rho_{\ell} \alpha_{\ell} v_{\ell}\right) g_x \end{bmatrix}. \tag{57}$$

Equivalently, we may express the model in full quasi-linear form

$$\frac{\partial \boldsymbol{U}}{\partial t} + \boldsymbol{A}(\boldsymbol{U}) \frac{\partial \boldsymbol{U}}{\partial x} = \boldsymbol{S}(\boldsymbol{U}), \tag{58}$$

where the Jacobian matrix $\boldsymbol{A}$ is given by

$$\mathbf{A}(\boldsymbol{U}) = [a_{ij}(\boldsymbol{U})] = \frac{\partial \boldsymbol{F}(\boldsymbol{U})}{\partial \boldsymbol{U}} + \mathbf{B}(\boldsymbol{U}) \frac{\partial \boldsymbol{W}(\boldsymbol{U})}{\partial \boldsymbol{U}}. \tag{59}$$

The relation

$$\mathrm{d}I_k = v_k \, \mathrm{d}m_k + m_k \, \mathrm{d}v_k, \tag{60}$$

allows us to obtain the differentials of the velocities of each phase as a function of the conserved variables:

$$\mathrm{d}v_{\mathrm{g}} = \frac{\mathrm{d}u_3 - v_{\mathrm{g}} \, \mathrm{d}u_1}{m_{\mathrm{g}}}, \tag{61}$$

$$\mathrm{d}v_{\ell} = \frac{\mathrm{d}u_4 - v_{\ell} \, \mathrm{d}u_2}{m_{\ell}}. \tag{62}$$

Herein, the variables I_k and m_k are defined in (56).

The two first rows of the Jacobian matrix corresponding to the mass conservation equations are easily determined with the information obtained so far. The analytical expressions corresponding to the three remaining rows, the two momentum and the energy equations, require further analysis. The third row, corresponding to the gas momentum equation, may be expressed as

$$a_{3j} = I_{\mathrm{g}} \frac{\partial v_{\mathrm{g}}}{\partial u_j} + v_{\mathrm{g}} \frac{\partial I_{\mathrm{g}}}{\partial u_j} + \Delta_{\mathrm{i}} p \frac{\partial \alpha_{\mathrm{g}}}{\partial u_j} + \alpha_{\mathrm{g}} \frac{\partial p}{\partial u_j}, \tag{63}$$

and a similar expression can be obtained for the liquid momentum equation

$$a_{4j} = I_{\ell} \frac{\partial v_{\ell}}{\partial u_j} + v_{\ell} \frac{\partial I_{\ell}}{\partial u_j} + \Delta_{\mathrm{i}} p \frac{\partial \alpha_{\ell}}{\partial u_j} + \alpha_{\ell} \frac{\partial p}{\partial u_j}. \tag{64}$$

The fifth row, associated to the total energy of the mixture, may be written as follows:

$$\begin{aligned} a_{5j} = {} & E_{\mathrm{g}} \frac{\partial v_{\mathrm{g}}}{\partial u_j} + v_{\mathrm{g}} \left\{ \left(e_{\mathrm{g}} + \frac{v_{\mathrm{g}}^2}{2} \right) \frac{\partial m_{\mathrm{g}}}{\partial u_j} + m_{\mathrm{g}} \left(\frac{\partial e_{\mathrm{g}}}{\partial u_j} + v_{\mathrm{g}} \frac{\partial v_{\mathrm{g}}}{\partial u_j} \right) \right\} \\ & + E_{\ell} \frac{\partial v_{\ell}}{\partial u_j} + v_{\ell} \left\{ \left(e_{\ell} + \frac{v_{\ell}^2}{2} \right) \frac{\partial m_{\ell}}{\partial u_j} + m_{\ell} \left(\frac{\partial e_{\ell}}{\partial u_j} + v_{\ell} \frac{\partial v_{\ell}}{\partial u_j} \right) \right\} \\ & + \left(\alpha_{\mathrm{g}} v_{\mathrm{g}} + \alpha_{\ell} v_{\ell} \right) \frac{\partial p}{\partial u_j} + p \left\{ \alpha_{\mathrm{g}} \frac{\partial v_{\mathrm{g}}}{\partial u_j} + \alpha_{\ell} \frac{\partial v_{\ell}}{\partial u_j} + \left(v_{\mathrm{g}} - v_{\ell} \right) \frac{\partial \alpha_{\mathrm{g}}}{\partial u_j} \right\}. \end{aligned} \tag{65}$$

Thus, additional relations must be found to determine the partial derivatives of p, α_k and e_k. In particular, two independent EOSes may be introduced:

$$\rho_k = \rho_k \left(T, p \right), \tag{66}$$

$$e_k = e_k \left(T, \rho_k \right), \tag{67}$$

along with their differentials

$$\mathrm{d}\rho_k = \left.\frac{\partial \rho_k}{\partial T}\right|_p \mathrm{d}T + \left.\frac{\partial \rho_k}{\partial p}\right|_T \mathrm{d}p, \tag{68}$$

$$\mathrm{d}e_k = \left.\frac{\partial e_k}{\partial T}\right|_{\rho_k} \mathrm{d}T + \left.\frac{\partial e_k}{\partial \rho_k}\right|_T \mathrm{d}\rho_k. \tag{69}$$

Herein, it will be convenient to use the simplified notation

$$\mathfrak{a}_k = \left.\frac{\partial \rho_k}{\partial T}\right|_p, \quad \mathfrak{b}_k = \left.\frac{\partial \rho_k}{\partial p}\right|_T, \quad \mathfrak{c}_k = \left.\frac{\partial e_k}{\partial T}\right|_{\rho_k}, \quad \mathfrak{d}_k = \left.\frac{\partial e_k}{\partial \rho_k}\right|_T. \tag{70}$$

Another equation to be used comes from $\mathrm{d}(\alpha_\mathrm{g} + \alpha_\ell) = 0$. In particular, the following notation has proved to be useful:

$$\frac{\mathrm{d}u_1}{\rho_\mathrm{g}} + \frac{\mathrm{d}u_2}{\rho_\ell} = q\,\mathrm{d}T + r\,\mathrm{d}p, \tag{71}$$

where

$$q = \sum_k \frac{\alpha_k \mathfrak{a}_k}{\rho_k}, \quad r = \sum_k \frac{\alpha_k \mathfrak{b}_k}{\rho_k}. \tag{72}$$

The last additional equation comes from the definition of the total energy of the mixture:

$$m_\mathrm{g}\,\mathrm{d}e_\mathrm{g} + m_\ell\,\mathrm{d}e_\ell = \left(\frac{v_\mathrm{g}^2}{2} - e_\mathrm{g}\right)\mathrm{d}u_1 + \left(\frac{v_\ell^2}{2} - e_\ell\right)\mathrm{d}u_2 - v_\mathrm{g}\,\mathrm{d}u_3 - v_\ell\,\mathrm{d}u_4 + \mathrm{d}u_5. \tag{73}$$

The resolution of the system of equations given by (68)–(69), (71) and (73) allows us to obtain expressions for the partial derivatives of the primitive variables ρ_g, ρ_ℓ, e_g, e_ℓ, T and p with respect to the conserved variables $\boldsymbol{U}$. The final result may be written, in the form of gradients, as follows:

$$\nabla_{\boldsymbol{U}} p = \tau^{-1} \begin{bmatrix} (v_\mathrm{g}^2/2 - e_\mathrm{g})q - \sum_k m_k \left(\mathfrak{a}_k \mathfrak{d}_k + \mathfrak{c}_k\right)/\rho_\mathrm{g} \\ (v_\ell^2/2 - e_\ell)q - \sum_k m_k \left(\mathfrak{a}_k \mathfrak{d}_k + \mathfrak{c}_k\right)/\rho_\ell \\ -v_\mathrm{g} q \\ -v_\ell q \\ q \end{bmatrix}, \tag{74}$$

$$\nabla_{\boldsymbol{U}} e_\mathrm{g} = \tau^{-1} \begin{bmatrix} (v_\mathrm{g}^2/2 - e_\mathrm{g})z_\mathrm{g} + \left(\mathfrak{d}_\mathrm{g}\mu + m_\ell \xi\right)/\rho_\mathrm{g} \\ (v_\ell^2/2 - e_\ell)z_\mathrm{g} + \left(\mathfrak{d}_\mathrm{g}\mu + m_\ell \xi\right)/\rho_\ell \\ -v_\mathrm{g} z_\mathrm{g} \\ -v_\ell z_\mathrm{g} \\ z_\mathrm{g} \end{bmatrix}, \tag{75}$$

$$\nabla_{\boldsymbol{U}} e_\ell = \tau^{-1} \begin{bmatrix} (v_\mathrm{g}^2/2 - e_\mathrm{g})z_\ell + \left(\mathfrak{d}_\ell \eta - m_\mathrm{g} \xi\right)/\rho_\mathrm{g} \\ (v_\ell^2/2 - e_\ell)z_\ell + \left(\mathfrak{d}_\ell \eta - m_\mathrm{g} \xi\right)/\rho_\ell \\ -v_\mathrm{g} z_\ell \\ -v_\ell z_\ell \\ z_\ell \end{bmatrix}, \tag{76}$$

$$\nabla_{\boldsymbol{U}} \rho_\mathrm{g} = \tau^{-1} \begin{bmatrix} (v_\mathrm{g}^2/2 - e_\mathrm{g})x_\mathrm{g} + \left(\mu - \mathfrak{b}_\mathrm{g} \sum_k m_k \mathfrak{c}_k\right)/\rho_\mathrm{g} \\ (v_\ell^2/2 - e_\ell)x_\mathrm{g} + \left(\mu - \mathfrak{b}_\mathrm{g} \sum_k m_k \mathfrak{c}_k\right)/\rho_\ell \\ -v_\mathrm{g} x_\mathrm{g} \\ -v_\ell x_\mathrm{g} \\ x_\mathrm{g} \end{bmatrix}. \tag{77}$$

where

$$\tau = -r \sum_k m_k \left(\mathfrak{a}_k \mathfrak{d}_k + \mathfrak{c}_k\right) + q \sum_k m_k \mathfrak{b}_k \mathfrak{d}_k, \tag{78}$$

$$x_k = -\mathfrak{a}_k r + \mathfrak{b}_k q, \tag{79}$$

$$z_k = -r \left(\mathfrak{a}_k \mathfrak{d}_k + \mathfrak{c}_k\right) + q \mathfrak{b}_k \mathfrak{d}_k, \tag{80}$$

$$\xi = \mathfrak{c}_{\mathrm{g}} \mathfrak{b}_\ell \mathfrak{d}_\ell - \mathfrak{c}_\ell \mathfrak{b}_{\mathrm{g}} \mathfrak{d}_{\mathrm{g}}, \tag{81}$$

$$\eta = m_{\mathrm{g}} \mathfrak{d}_{\mathrm{g}} \left(\mathfrak{a}_\ell \mathfrak{b}_{\mathrm{g}} - \mathfrak{a}_{\mathrm{g}} \mathfrak{b}_\ell\right), \tag{82}$$

$$\mu = m_\ell \mathfrak{d}_\ell \left(\mathfrak{a}_{\mathrm{g}} \mathfrak{b}_\ell - \mathfrak{a}_\ell \mathfrak{b}_{\mathrm{g}}\right). \tag{83}$$

The partial derivatives of the gas volume fraction with respect to the conserved variables can be written as

$$\nabla_{\boldsymbol{U}} \alpha_{\mathrm{g}} = -\nabla_{\boldsymbol{U}} \alpha_\ell = \frac{\mathrm{d}u_1}{\rho_{\mathrm{g}}} \begin{bmatrix} 1 \\ 0 \\ 0 \\ 0 \\ 0 \end{bmatrix} - \frac{\alpha_{\mathrm{g}}}{\rho_{\mathrm{g}}} \nabla_{\boldsymbol{U}} \rho_{\mathrm{g}}. \tag{84}$$

Further simplifications can be introduced for the derivatives of the primitive variables. In particular, we know that p, e_k and ρ_{g} do not depend on the velocity and consequently they can be expressed in terms of a *reduced* set of conserved variables given by

$$\boldsymbol{\Omega} = \begin{bmatrix} m_{\mathrm{g}} \\ m_\ell \\ m_{\mathrm{g}} e_{\mathrm{g}} + m_\ell e_\ell \end{bmatrix}. \tag{85}$$

Thus $\mathrm{d}p$, $\mathrm{d}e_k$ and $\mathrm{d}\rho_{\mathrm{g}}$ may be written as

$$\mathrm{d}(\cdot) = \sum_{j=1}^{5} \frac{\partial(\cdot)}{\partial u_j} \mathrm{d}u_j = \sum_{j=1}^{3} \frac{\partial(\cdot)}{\partial \omega_j} \mathrm{d}\omega_j, \tag{86}$$

where the differentials $\mathrm{d}\omega_1$ and $\mathrm{d}\omega_2$ satisfy

$$\mathrm{d}\omega_1 = \mathrm{d}u_1, \quad \mathrm{d}\omega_2 = \mathrm{d}u_2. \tag{87}$$

By rewriting (73) we can relate $\mathrm{d}\omega_3$ to the differentials of the conserved variables

$$\mathrm{d}\omega_3 = \frac{v_{\mathrm{g}}^2}{2} \mathrm{d}u_1 + \frac{v_\ell^2}{2} \mathrm{d}u_2 - v_{\mathrm{g}} \mathrm{d}u_3 - v_\ell \mathrm{d}u_4 + \mathrm{d}u_5. \tag{88}$$

Relations (86)–(88) allow us to express the partial derivatives of p, e_k and ρ_g with respect to the reduced variables:

$$\frac{\partial(\cdot)}{\partial u_1} = \frac{\partial(\cdot)}{\partial \omega_1} + \frac{v_\mathrm{g}^2}{2}\frac{\partial(\cdot)}{\partial \omega_3}, \tag{89}$$

$$\frac{\partial(\cdot)}{\partial u_2} = \frac{\partial(\cdot)}{\partial \omega_2} + \frac{v_\ell^2}{2}\frac{\partial(\cdot)}{\partial \omega_3}, \tag{90}$$

$$\frac{\partial(\cdot)}{\partial u_3} = -v_\mathrm{g}\frac{\partial(\cdot)}{\partial \omega_3}, \tag{91}$$

$$\frac{\partial(\cdot)}{\partial u_4} = -v_\ell\frac{\partial(\cdot)}{\partial \omega_3}, \tag{92}$$

$$\frac{\partial(\cdot)}{\partial u_5} = \frac{\partial(\cdot)}{\partial \omega_3}. \tag{93}$$

In the following we will use the notation $\partial_j(\cdot) = \partial(\cdot)/\partial\omega_j$ to refer to these derivatives.

Now it is possible to fully determine the Jacobian matrix. This matrix has been split into convective, volume-fraction, energy and pressure parts as follows:

$$\mathbf{A} = \mathbf{A}_c + \mathbf{A}_\alpha + \mathbf{A}_e + \mathbf{A}_p. \tag{94}$$

Herein, the partial matrices satisfy

$$\mathbf{A}_c = \frac{\partial}{\partial \boldsymbol{U}}\begin{bmatrix} \rho_\mathrm{g}\alpha_\mathrm{g}v_\mathrm{g} \\ \rho_\ell\alpha_\ell v_\ell \\ \rho_\mathrm{g}\alpha_\mathrm{g}v_\mathrm{g}^2 \\ \rho_\ell\alpha_\ell v_\ell^2 \\ \frac{1}{2}\rho_\mathrm{g}\alpha_\mathrm{g}v_\mathrm{g}^3 + \frac{1}{2}\rho_\ell\alpha_\ell v_\ell^3 \end{bmatrix} + \begin{bmatrix} 0 & 0 & 0 & 0 \\ 0 & 0 & 0 & 0 \\ 0 & 0 & 0 & 0 \\ 0 & 0 & 0 & 0 \\ 0 & 0 & p\alpha_\mathrm{g} & p\alpha_\ell \end{bmatrix}\frac{\partial \boldsymbol{\Psi}}{\partial \boldsymbol{U}} + \begin{bmatrix} 0 & 0 & 0 & 0 & 0 \\ 0 & 0 & 0 & 0 & 0 \\ 0 & 0 & 0 & 0 & 0 \\ 0 & 0 & 0 & 0 & 0 \\ 0 & 0 & e_\mathrm{g} & e_\ell & 0 \end{bmatrix}\frac{\partial \boldsymbol{U}}{\partial \boldsymbol{U}}, \tag{95}$$

$$\mathbf{A}_\alpha = \begin{bmatrix} 0 \\ 0 \\ \Delta_\mathrm{i}p \\ -\Delta_\mathrm{i}p \\ p(v_\mathrm{g} - v_\ell) \end{bmatrix}\frac{\partial \alpha_\mathrm{g}}{\partial \boldsymbol{U}}, \qquad \mathbf{A}_e = \begin{bmatrix} 0 & 0 & 0 & 0 \\ 0 & 0 & 0 & 0 \\ 0 & 0 & 0 & 0 \\ 0 & 0 & 0 & 0 \\ \rho_\mathrm{g}\alpha_\mathrm{g}v_\mathrm{g} & \rho_\ell\alpha_\ell v_\ell & 0 & 0 \end{bmatrix}\frac{\partial \boldsymbol{\Psi}}{\partial \boldsymbol{U}}, \qquad \mathbf{A}_p = \begin{bmatrix} 0 \\ 0 \\ \alpha_\mathrm{g} \\ \alpha_\ell \\ \alpha_\mathrm{g}v_\mathrm{g} + \alpha_\ell v_\ell \end{bmatrix}\frac{\partial p}{\partial \boldsymbol{U}}, \tag{96}$$

where

$$\boldsymbol{\Psi}(\boldsymbol{U}) = \begin{bmatrix} e_\mathrm{g} \\ e_\ell \\ v_\mathrm{g} \\ v_\ell \end{bmatrix}. \tag{97}$$

The convective matrix may be written as

$$\mathbf{A}_c = \begin{bmatrix} 0 & 0 & 1 & 0 & 0 \\ 0 & 0 & 0 & 1 & 0 \\ -v_\mathrm{g}^2 & 0 & 2v_\mathrm{g} & 0 & 0 \\ 0 & -v_\ell^2 & 0 & 2v_\ell & 0 \\ -v_\mathrm{g}^3 - pv_\mathrm{g}/\rho_\mathrm{g} & -v_\ell^3 - pv_\ell/\rho_\ell & e_\mathrm{g} + 3v_\mathrm{g}^2/2 + p/\rho_\mathrm{g} & e_\ell + 3v_\ell^2/2 + p/\rho_\ell & 0 \end{bmatrix}, \tag{98}$$

whereas the volume-fraction matrix can be expressed as

$$\mathbf{A}_\alpha = \frac{\Delta_\mathrm{i}p\alpha_\mathrm{g}}{\rho_\mathrm{g}}\mathbf{A}_{\alpha_1} - \frac{p\left(v_\mathrm{g} - v_\ell\right)\alpha_\mathrm{g}}{\rho_\mathrm{g}}\mathbf{A}_{\alpha_2}, \tag{99}$$

with

$$\mathbf{A}_{\alpha_1} = \begin{bmatrix} 0 & 0 & 0 & 0 & 0 \\ 0 & 0 & 0 & 0 & 0 \\ 1/\alpha_{\mathrm{g}} - (\partial_1\rho_{\mathrm{g}} + v_{\mathrm{g}}^2/2\partial_3\rho_{\mathrm{g}}) & -(\partial_2\rho_{\mathrm{g}} + v_\ell^2/2\partial_3\rho_{\mathrm{g}}) & v_{\mathrm{g}}\partial_3\rho_{\mathrm{g}} & v_\ell\partial_3\rho_{\mathrm{g}} & -\partial_3\rho_{\mathrm{g}} \\ \partial_1\rho_{\mathrm{g}} + v_{\mathrm{g}}^2/2\partial_3\rho_{\mathrm{g}} - 1/\alpha_{\mathrm{g}} & \partial_2\rho_{\mathrm{g}} + v_\ell^2/2\partial_3\rho_{\mathrm{g}} & -v_{\mathrm{g}}\partial_3\rho_{\mathrm{g}} & -v_\ell\partial_3\rho_{\mathrm{g}} & \partial_3\rho_{\mathrm{g}} \\ 0 & 0 & 0 & 0 & 0 \end{bmatrix}, \tag{100}$$

and

$$\mathbf{A}_{\alpha_2} = \begin{bmatrix} 0 & 0 & 0 & 0 & 0 \\ 0 & 0 & 0 & 0 & 0 \\ 0 & 0 & 0 & 0 & 0 \\ 0 & 0 & 0 & 0 & 0 \\ \partial_1\rho_{\mathrm{g}} + v_{\mathrm{g}}^2/2\partial_3\rho_{\mathrm{g}} - 1/\alpha_{\mathrm{g}} & \partial_2\rho_{\mathrm{g}} + v_\ell^2/2\partial_3\rho_{\mathrm{g}} & -v_{\mathrm{g}}\partial_3\rho_{\mathrm{g}} & -v_\ell\partial_3\rho_{\mathrm{g}} & \partial_3\rho_{\mathrm{g}} \end{bmatrix}. \tag{101}$$

The energy matrix will be given by

$$\mathbf{A}_e = \begin{bmatrix} 0 & 0 & 0 & 0 & 0 \\ 0 & 0 & 0 & 0 & 0 \\ 0 & 0 & 0 & 0 & 0 \\ 0 & 0 & 0 & 0 & 0 \\ a_{e_1} & a_{e_2} & -v_{\mathrm{g}}a_{e_5} & -v_\ell a_{e_5} & a_{e_5} \end{bmatrix}, \tag{102}$$

where

$$a_{e_1} = \sum_k I_k \left(\frac{\partial e_k}{\partial \omega_1} + \frac{v_{\mathrm{g}}^2}{2} \frac{\partial e_k}{\partial \omega_3} \right), \tag{103}$$

$$a_{e_2} = \sum_k I_k \left(\frac{\partial e_k}{\partial \omega_2} + \frac{v_\ell^2}{2} \frac{\partial e_k}{\partial \omega_3} \right), \tag{104}$$

$$a_{e_5} = \sum_k I_k \frac{\partial e_k}{\partial \omega_3}. \tag{105}$$

Finally, the pressure matrix may be written as

$$\mathbf{A}_p = \begin{bmatrix} 0 & 0 & 0 & 0 & 0 \\ 0 & 0 & 0 & 0 & 0 \\ \alpha_{\mathrm{g}}(\partial_1 p + v_{\mathrm{g}}^2/2\partial_3 p) & \alpha_{\mathrm{g}}(\partial_2 p + v_\ell^2/2\partial_3 p) & -\alpha_{\mathrm{g}}v_{\mathrm{g}}\partial_3 p & -\alpha_{\mathrm{g}}v_\ell\partial_3 p & \alpha_{\mathrm{g}}\partial_3 p \\ \alpha_\ell(\partial_1 p + v_{\mathrm{g}}^2/2\partial_3 p) & \alpha_\ell(\partial_2 p + v_\ell^2/2\partial_3 p) & -\alpha_\ell v_{\mathrm{g}}\partial_3 p & -\alpha_\ell v_\ell\partial_3 p & \alpha_\ell\partial_3 p \\ v_{\mathrm{m}}(\partial_1 p + v_{\mathrm{g}}^2/2\partial_3 p) & v_{\mathrm{m}}(\partial_2 p + v_\ell^2/2\partial_3 p) & -v_{\mathrm{m}}v_{\mathrm{g}}\partial_3 p & -v_{\mathrm{m}}v_\ell\partial_3 p & v_{\mathrm{m}}\partial_3 p \end{bmatrix}, \tag{106}$$

where $v_{\mathrm{m}} = \alpha_{\mathrm{g}}v_{\mathrm{g}} + \alpha_\ell v_\ell$.

3.4.1. *Eigenstructure*

In this section, we derive analytical eigenvalues for the TF$_5$ model for the special case where the velocities of both phases are equal. In this case, the notation utilized to define the Jacobian matrix has proved to be convenient. Note in particular that if $v_{\mathrm{g}} = v_\ell = v$, then the convective matrix can be simplified into

$$\mathbf{A}_c = \begin{bmatrix} 0 & 0 & 1 & 0 & 0 \\ 0 & 0 & 0 & 1 & 0 \\ -v^2 & 0 & 2v & 0 & 0 \\ 0 & -v^2 & 0 & 2v & 0 \\ -v^3 - pv/\rho_{\mathrm{g}} & -v^3 - pv/\rho_\ell & e_{\mathrm{g}} + 3v^2/2 + p/\rho_{\mathrm{g}} & e_\ell + 3v^2/2 + p/\rho_\ell & 0 \end{bmatrix}, \tag{107}$$

whereas the energy matrix can be reduced to

$$\mathbf{A}_e = \begin{bmatrix} 0 & 0 & 0 & 0 & 0 \\ 0 & 0 & 0 & 0 & 0 \\ 0 & 0 & 0 & 0 & 0 \\ 0 & 0 & 0 & 0 & 0 \\ v(v^2/2 - e_{\mathrm{g}}) & v(v^2/2 - e_{\ell}) & -v^2 & -v^2 & v \end{bmatrix}, \tag{108}$$

and the pressure matrix into

$$\mathbf{A}_p = \begin{bmatrix} 0 & 0 & 0 & 0 & 0 \\ 0 & 0 & 0 & 0 & 0 \\ \alpha_{\mathrm{g}}(\partial_1 p + v^2/2\partial_3 p) & \alpha_{\mathrm{g}}(\partial_2 p + v^2/2\partial_3 p) & -v\alpha_{\mathrm{g}}\partial_3 p & -v\alpha_{\mathrm{g}}\partial_3 p & \alpha_{\mathrm{g}}\partial_3 p \\ \alpha_{\ell}(\partial_1 p + v^2/2\partial_3 p) & \alpha_{\ell}(\partial_2 p + v^2/2\partial_3 p) & -v\alpha_{\ell}\partial_3 p & -v\alpha_{\ell}\partial_3 p & \alpha_{\ell}\partial_3 p \\ v(\partial_1 p + v^2/2\partial_3 p) & v(\partial_2 p + v^2/2\partial_3 p) & -v^2\partial_3 p & -v^2\partial_3 p & v\partial_3 p \end{bmatrix}. \tag{109}$$

The characteristic polynomial of the Jacobian matrix $\mathbf{A} = \mathbf{A}_c + \mathbf{A}_e + \mathbf{A}_p$ may be written as

$$\lambda^5 - 5v\lambda^4 + \left(10v^2 - c^2_{\mathrm{TF}_5}\right)\lambda^3 + \left(3vc^2_{\mathrm{TF}_5} - 10v^3\right)\lambda^2 + \left(5v^4 - 3v^2c^2_{\mathrm{TF}_5}\right)\lambda \ + v^3c^2_{\mathrm{TF}_5} - v^5 = 0, \tag{110}$$

where

$$c^2_{\mathrm{TF}_5} = \sum_{j=1}^{2} \alpha_j \frac{\partial p}{\partial \omega_j} + \sum_{j=1}^{2} \alpha_j \left(e_j + \frac{p}{\rho_j}\right) \frac{\partial p}{\partial \omega_3}. \tag{111}$$

Consequently, the eigenvalues will be given by

$$\mathbf{\Lambda}_{\mathrm{TF}_5} = \begin{bmatrix} v - c_{\mathrm{TF}_5} \\ v \\ v \\ v \\ v + c_{\mathrm{TF}_5} \end{bmatrix}, \tag{112}$$

where c_{TF_5} is the speed of sound of the five-equation two-fluid model, assuming equal velocities in both phases. Herein, the subscripts $j = 1 \equiv \mathrm{g}$ and $j = 2 \equiv \ell$ have been utilized. Following the arguments of [15,41], one may expect the expression (111) to be a good approximation to the sound velocity also for more general cases where $v_{\mathrm{g}} \neq v_{\ell}$.

When we assume the equations of state (66)–(67), the expression (111) may be rewritten in a more convenient form. To this end, we take advantage of the internal-energy differential given in [17]:

$$\mathrm{d}(\rho e) = \sum_{j=1}^{2} \left(e_j + \frac{p}{\rho_j}\right) \mathrm{d}u_j - T\frac{\sum_k C_{p,k}}{\sum_k \zeta_k C_{p,k}} \sum_{j=1}^{2} \frac{\mathrm{d}u_j}{\rho_j} + \frac{T}{\rho c^2_{\mathrm{DF}_4}} \frac{\sum_k C_{p,k}}{\sum_k \zeta_k C_{p,k}} \mathrm{d}p, \tag{113}$$

where

$$\rho = \rho_{\mathrm{g}}\alpha_{\mathrm{g}} + \rho_{\ell}\alpha_{\ell} = \omega_1 + \omega_2 \tag{114}$$

and

$$\rho e = \rho_{\mathrm{g}}\alpha_{\mathrm{g}}e_{\mathrm{g}} + \rho_{\ell}\alpha_{\ell}e_{\ell} = \omega_3 \tag{115}$$

are the total volumetric mass and the internal energy of the system, respectively.

The differential of the pressure can be isolated from (113) and written in terms of the reduced variables:

$$\mathrm{d}p = \rho c^2_{\mathrm{DF}_4} \sum_{j=1}^{2} \frac{\mathrm{d}\omega_j}{\rho_j} + \frac{\rho c^2_{\mathrm{DF}_4}}{T} \frac{\sum_k \zeta_k C_{p,k}}{\sum_k C_{p,k}} \left\{ \mathrm{d}\omega_3 - \sum_{j=1}^{2} \left(e_j + \frac{p}{\rho_j}\right) \mathrm{d}\omega_j \right\}. \tag{116}$$

Using (116) to obtain the partial derivatives of the pressure and substituting them in (111) leads us to the relation

$$c^2_{\text{TF}_5} = \rho \left(\frac{\alpha_{\text{g}}}{\rho_{\text{g}}} + \frac{\alpha_\ell}{\rho_\ell} \right) c^2_{\text{DF}_4}, \tag{117}$$

where c_{DF_4} is given by (52).

4. The Subcharacteristic Condition

In this section, we demonstrate that the relaxation processes we are considering in this paper satisfy a subcharacteristic condition. We start by making the following observation:

Proposition 1. *The relative effect our relaxation processes have on sonic propagation is independent of the order in which the relaxation processes are being performed, in the following precise sense:*

$$\frac{c_{\text{TF}_5}}{c_{\text{DF}_4}} = \frac{c_{\text{TF}_6}}{c_{\text{DF}_5}} \tag{118}$$

and

$$\frac{c_{\text{TF}_6}}{c_{\text{TF}_5}} = \frac{c_{\text{DF}_5}}{c_{\text{DF}_4}}. \tag{119}$$

Proof. By comparing (50) to (47) we obtain:

$$c^2_{\text{TF}_6} = \rho \left(\frac{\alpha_{\text{g}}}{\rho_{\text{g}}} + \frac{\alpha_\ell}{\rho_\ell} \right) c^2_{\text{DF}_5}, \tag{120}$$

from which (118) follows from (117). Then (119) follows directly from (118). □

We now state a weaker version of the subcharacteristic condition given by Definition 1:

Definition 6. *Let the M eigenvalues of the relaxation system* (1) *be given by*

$$\lambda_1 \leq \ldots \leq \lambda_k \leq \lambda_{k+1} \leq \ldots \leq \lambda_M \tag{121}$$

and the N eigenvalues of the relaxed system (4)–(6) *be given by*

$$\tilde{\lambda}_1 \leq \ldots \leq \tilde{\lambda}_j \leq \tilde{\lambda}_{j+1} \leq \ldots \leq \tilde{\lambda}_N. \tag{122}$$

Now let $\tilde{\mathcal{M}}$ be a second Maxwellian operator $\tilde{\mathcal{M}} : \tilde{\Omega} \subseteq \mathbb{R}^K \mapsto \mathbb{R}^N$, where $K < N$.

Herein, the relaxation systems (1) *and* (6) *are applied to local equilibrium states $\boldsymbol{U}$ and $\boldsymbol{V}$ given by*

$$\boldsymbol{V} = \tilde{\mathcal{M}}(\boldsymbol{W}), \qquad \boldsymbol{U} = \mathcal{M}(\boldsymbol{V}) \tag{123}$$

such that

$$\lambda_k = \lambda_k(\mathcal{M}(\tilde{\mathcal{M}}(\boldsymbol{W}))), \qquad \tilde{\lambda}_j = \tilde{\lambda}_j(\tilde{\mathcal{M}}(\boldsymbol{W})). \tag{124}$$

Now let the $\tilde{\lambda}_j$ be interlaced *with λ_k in the following sense: Each $\tilde{\lambda}_j$ lies in the closed interval $[\lambda_j, \lambda_{j+M-N}]$ for all $\boldsymbol{W} \in \tilde{\Omega}$. Then the relaxed system* (6) *is said to satisfy a* **weak subcharacteristic condition** *with respect to* (1) *and $\tilde{\Omega}$.*

Using Definitions 1 and 6, we may now state some results.

Proposition 2. *The relaxation models we are considering in this paper are related as follows:*

SC1: *The model* DF_4 *satisfies the subcharacteristic condition with respect to* DF_5.

SC2: *The model* DF_4 *satisfies the subcharacteristic condition with respect to* TF_5.

SC3: *The model* DF_5 *satisfies the subcharacteristic condition with respect to* TF_6.
SC4: *The model* TF_5 *satisfies the weak subcharacteristic condition with respect to the model* TF_6 *and the equilibria given by solutions of* DF_4.

Proof. SC1 was proved in [17]. By inspection of (49), (51), (48), (112), and Definitions 1 and 6, we see that SC2–SC4 hold provided

$$c_{\mathrm{TF}_5} \geq c_{\mathrm{DF}_4}, \tag{125}$$
$$c_{\mathrm{TF}_6} \geq c_{\mathrm{DF}_5}, \tag{126}$$
$$c_{\mathrm{TF}_6} \geq c_{\mathrm{TF}_5}. \tag{127}$$

From (117) and (118) we see that (125)–(126) hold provided

$$\rho \left(\frac{\alpha_\mathrm{g}}{\rho_\mathrm{g}} + \frac{\alpha_\ell}{\rho_\ell} \right) \geq 1, \tag{128}$$

which by (114) can be written as

$$\alpha_\ell^2 \left(2 - \frac{\rho_\mathrm{g}}{\rho_\ell} - \frac{\rho_\ell}{\rho_\mathrm{g}} \right) - \alpha_\ell \left(2 - \frac{\rho_\mathrm{g}}{\rho_\ell} - \frac{\rho_\ell}{\rho_\mathrm{g}} \right) \geq 0. \tag{129}$$

In particular, this holds if

$$2 - \frac{\rho_\mathrm{g}}{\rho_\ell} - \frac{\rho_\ell}{\rho_\mathrm{g}} \leq 0. \tag{130}$$

Multiplying (130) by $\rho_\mathrm{g}/\rho_\ell$, which is always a positive quantity, we can finally simplify this expression into

$$\left(\frac{\rho_\mathrm{g}}{\rho_\ell} - 1 \right)^2 \geq 0 \tag{131}$$

and therefore (125)–(126) hold. Finally, (127) follows from (52) and (119). □

We remark that since the subcharacteristic condition is essential for linear stability, we expect SC4 to hold also in the strong sense of Definition 1. However, addressing this question with a direct algebraic approach will run into difficulties as described in [15, 41]. It is possible that an analysis based on more general arguments, following for instance ideas of Chen *et al.* [8], may be more fruitful. We will not pursue this issue further in our current paper.

In the following sections, we will demonstrate how the above results manifest themselves in some concrete two-phase mixtures of practical relevance.

4.1. **Water-Air under Atmospheric Conditions**

We first consider a state representing a mixture of water and air under atmospheric conditions, where the thermodynamic parameters are given by Table 1. Numerical values as a function of the liquid volume fraction are plotted in Figure 1. Herein, Figure 1(a) shows the mixture sonic velocities of the various models. The subcharacteristic conditions of Proposition 2 are verified by the plot, and we observe that velocity relaxation has a bigger impact than temperature relaxation on the mixture sound velocity.

In Figure 1(b), the ratio of the sound velocities given by the models with and without temperature relaxation are plotted as a function of the liquid volume fraction. The plot illustrates the relation (119), and we observe that the sound velocities differ by approximately 18 % except near the single-phase regions.

TABLE 1. Water-air mixture under atmospheric conditions.

Quantity	gas (air)	liquid (water)
Pressure (MPa)	0.1	0.1
Temperature (K)	308.15	308.15
Density (kg/m^3)	1.0984	1000.0
Sound speed (m/s)	357.01	1542.8
c_p (J/(kg $\cdot$ K))	1008.7	4186.0
ζ (1×10^{-7} (m $\cdot$ s^2 $\cdot$ K)/kg)	9025.7	2.3889

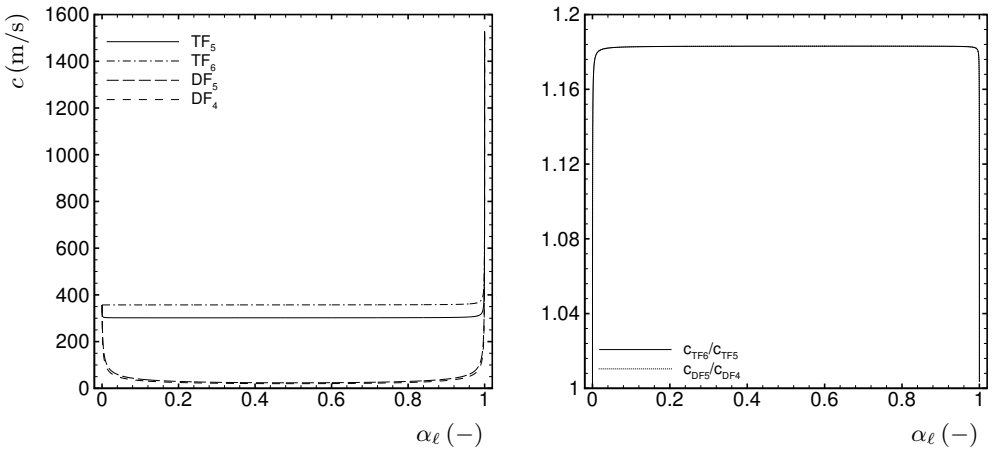

(a) Speed of sound. (b) Speed of sound (ratio).

FIGURE 1. Water-air mixture under atmospheric conditions. Speed of sound for the considered two-phase flow models (a) and their corresponding ratios (b).

TABLE 2. Water-air mixture under high pressure.

Quantity	gas (air)	liquid (water)
Pressure (MPa)	20	20
Temperature (K) (K)	308.15	308.15
Density (kg/m^3)	225.20	1049.2
Sound speed (m/s)	352.61	1523.8
c_p (J/(kg $\cdot$ K))	1008.7	4186.0
ζ (1×10^{-7} (m $\cdot$ s^2 $\cdot$ K)/kg)	44.021	2.2770

4.2. **Water-Air under High Pressure**

We now consider a state representing a rough approximation to a water-air mixture under high pressure, forming the basis for the numerical simulations presented in Section 6.2. The thermodynamic parameters are given in Table 2. The speed of sound as a function of the liquid volume fraction is plotted in Figure 2. Figure 2(a) illustrates the inequalities of Proposition 2. Note that the curves of c_{TF_5} and c_{DF_5} intersect; as these models are not related through a relaxation procedure, they do not satisfy a subcharacteristic inequality.

Figure 2(b) indicates that the relative effect of thermal relaxation on sonic propagation is somewhat weakened as the pressure is increased compared to Section 4.1.

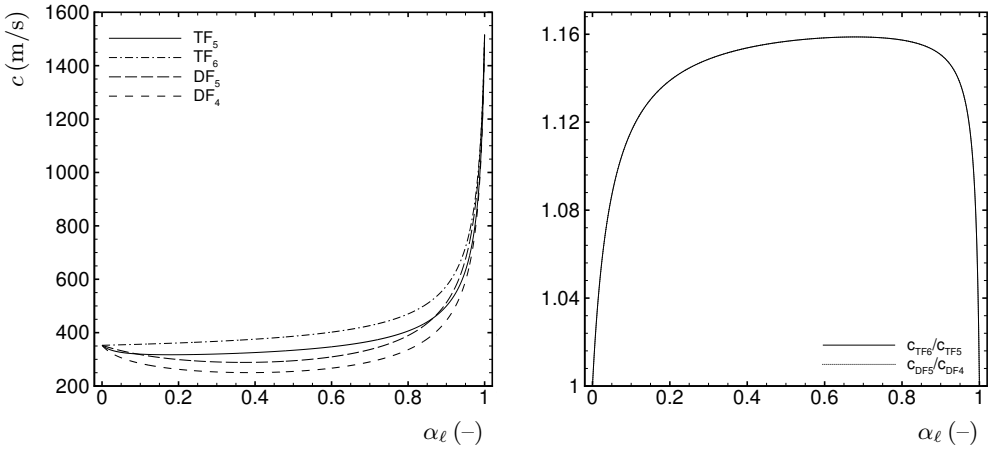

(a) Speed of sound. (b) Speed of sound (ratio).

FIGURE 2. Water-air mixture under high pressure. Speed of sound for the considered two-phase flow models (a) and their corresponding ratios (b).

TABLE 3. Two-Phase CO_2 Mixture.

Quantity	gas (CO_2)	liquid (CO_2)
Pressure (MPa)	5	5
Temperature (K) (K)	273	273
Density (kg/m^3)	117.70	1000.0
Sound speed (m/s)	227.75	522.49
c_p (J/(kg $\cdot$ K))	1900	2500
ζ (1×10^{-7} (m $\cdot$ s^2 $\cdot$ K)/kg)	44.717	4

4.3. **A Two-Phase CO_2 Mixture**

As our final illustration, we consider a mixture of CO_2 in its gas and liquid state. The thermodynamic parameters are given in Table 3. The sound velocities and their ratios are plotted in Figure 3. Note that in this case, the mixture sound velocities vary with at most 4 % between the thermally relaxed and non-relaxed models, a much smaller difference than for the water-air mixture considered above. An interpretation of these results will be provided in the following.

4.3.1. *Theoretical Considerations*

We observe from (50) and (52) that the speed of sound ratio for thermal relaxation can be written as

$$\left(\frac{c_{\mathrm{TF}_6}}{c_{\mathrm{TF}_5}}\right)^2 = \left(\frac{c_{\mathrm{DF}_5}}{c_{\mathrm{DF}_4}}\right)^2 = 1 + \left(\frac{\alpha_\mathrm{g}}{\rho_\mathrm{g} c_\mathrm{g}^2} + \frac{\alpha_\ell}{\rho_\ell c_\ell^2}\right)^{-1} \frac{C_{p,\mathrm{g}} C_{p,\ell} (\zeta_\mathrm{g} - \zeta_\ell)^2}{(C_{p,\mathrm{g}} + C_{p,\ell}) T}. \tag{132}$$

Furthermore, the parameter ζ can be expressed in terms of the dimensionless Grüneisen coefficient defined in (25):

$$\zeta_k = \frac{T_k}{\rho_k c_k^2} \Gamma_k. \tag{133}$$

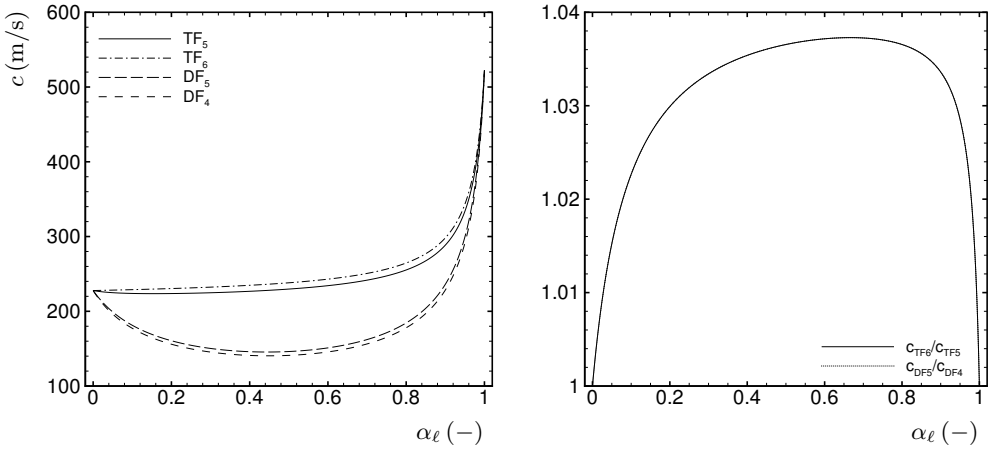

(a) Speed of sound. (b) Speed of sound (ratio).

FIGURE 3. Two-phase CO_2 mixture. Speed of sound for the considered two-phase flow models (a) and their corresponding ratios (b).

Hence in thermal equilibrium, (132) can be written as

$$\left(\frac{c_{\mathrm{TF}_6}}{c_{\mathrm{TF}_5}}\right)^2 = \left(\frac{c_{\mathrm{DF}_5}}{c_{\mathrm{DF}_4}}\right)^2 = 1 + T\left(\frac{\alpha_\mathrm{g}}{\rho_\mathrm{g} c_\mathrm{g}^2} + \frac{\alpha_\ell}{\rho_\ell c_\ell^2}\right)^{-1}\left(\frac{\Gamma_\mathrm{g}}{\rho_\mathrm{g} c_\mathrm{g}^2} - \frac{\Gamma_\ell}{\rho_\ell c_\ell^2}\right)^2 \frac{C_{p,\mathrm{g}} C_{p,\ell}}{C_{p,\mathrm{g}} + C_{p,\ell}}. \tag{134}$$

As the Grüneisen coefficient will generally be close to unity, this result suggests that the ratio

$$\mathcal{R} = \frac{\rho_\ell c_\ell^2}{\rho_\mathrm{g} c_\mathrm{g}^2} \tag{135}$$

is a main parameter influencing the effect of thermal relaxation on the velocity of pressure waves. This largely explains the observations made in Sections 4.2–4.3.

5. An Approximate Riemann Solver

With the aid of the results obtained in Section 3.4, we here derive a simple linearized approximate Riemann solver for the TF$_5$ model. According to Roe [33], solving the nonlinear problem (55) requires introducing a local linearization

$$\frac{\partial \boldsymbol{U}}{\partial t} + \hat{\mathbf{A}}_{i-1/2}(\boldsymbol{U}_{i-1}, \boldsymbol{U}_i)\frac{\partial \boldsymbol{U}}{\partial x} = \boldsymbol{S}(\boldsymbol{U}), \tag{136}$$

where the matrix $\hat{\mathbf{A}}_{i-1/2}(\boldsymbol{U}_{i-1}, \boldsymbol{U}_i)$, known as the Roe matrix, is some averaged Jacobian matrix depending on the states $\boldsymbol{U}_{i-1}$ and $\boldsymbol{U}_i$. This matrix must satisfy the following properties, also known as the Roe conditions:

- R1: $\hat{\mathbf{A}}_{i-1/2}$ must retain the hyperbolicity of the system. The Roe matrix is diagonalizable with real eigenvalues.
- R2: $\hat{\mathbf{A}}_{i-1/2}$ must be consistent with the exact Jacobian, that is $\hat{\mathbf{A}}_{i-1/2}(\boldsymbol{U}, \boldsymbol{U}) = \mathbf{A}(\boldsymbol{U})$.
- R3: $\hat{\mathbf{A}}_{i-1/2}$ is conservative across discontinuities: $\hat{\mathbf{A}}_{i-1/2}(\boldsymbol{U}_i - \boldsymbol{U}_{i-1}) = \boldsymbol{F}(\boldsymbol{U}_i) - \boldsymbol{F}(\boldsymbol{U}_{i-1})$.

As can be seen from the analysis of Section 3.4, the Jacobian involves a complicated interplay between the fluid-mechanical and thermodynamic variables of the system, rendering the parameter-vector approach suggested by Roe [33] impractical. Instead we will follow an approach based on direct algebraic manipulation,

splitting the problem into subproblems that may be solved largely by simple arithmetic averages. In this respect, our linearization will be heavily *quasi-Jacobian* in the terminology of [9].

This has some disadvantages; in particular, we *cannot* write the Roe matrix in the form

$$\hat{\mathbf{A}}_{i-1/2}(\boldsymbol{U}_{i-1},\boldsymbol{U}_i) = \mathbf{A}(\hat{\boldsymbol{U}}_{i-1/2}(\boldsymbol{U}_{i-1},\boldsymbol{U}_i)), \tag{137}$$

as would have been the case with the more formal parameter-vector approach. Although this has no impact on the conditions R2 and R3, we now cannot prove that our Roe matrix satisfies the condition R1. However, no violation of R1 was observed for any of the simulations presented in this paper. Hence our simplified approach serves our current purpose, and allows us to perform high-resolution upwind calculations to study the properties of the model.

However, we remark that a finer analysis may lead to a formulation of a Roe matrix that is more consistent with the true Jacobian of the TF_5 model. This will not be pursued further in the present paper.

5.1. **A Non-Conservative Formulation**

An additional complication arises from the fact that the system (55) is *nonconservative* and therefore a generalization of the condition R3 is needed [40, 41]. It is convenient to introduce the operator $\Delta(\cdot)$ to indicate a *jump* in a variable. Thus, the third condition of Roe can be written as

$$\hat{\mathbf{A}}_{i-1/2}\Delta\boldsymbol{U} = \Delta\boldsymbol{F}. \tag{138}$$

The non-conservative modification to this becomes

$$\hat{\mathbf{A}}_{i-1/2}\Delta\boldsymbol{U} = \Delta\boldsymbol{F} + \overline{\overline{\mathbf{B}}}_{i-1/2}\Delta\boldsymbol{W}, \tag{139}$$

which is the averaged version of

$$\int_{\boldsymbol{U}_{i-1}}^{\boldsymbol{U}_i} \boldsymbol{A}(\boldsymbol{U})\,\mathrm{d}\boldsymbol{U} = \Delta\boldsymbol{F} + \int_{\boldsymbol{U}_{i-1}}^{\boldsymbol{U}_i} \boldsymbol{B}(\boldsymbol{U})\nabla_{\boldsymbol{U}}\boldsymbol{W}\,\mathrm{d}\boldsymbol{U} \tag{140}$$

along some path connecting $\boldsymbol{U}_{i-1}$ and $\boldsymbol{U}_i$.

In this work, we will follow the simplified approach used for instance in [27], where $\overline{\overline{\mathbf{B}}}_{i-1/2}$ is obtained from algebraic averaging rather than integrating over a path. Our analysis will be based on the rather extensive decomposition (95)–(96). In this respect, we remark that our Roe matrix is unlikely to represent an average over an explicit path integral of the form (140).

Note that the Roe matrix corresponds to an averaged Jacobian matrix between two neighbouring cells, and to find it, we have to repeat the procedure described in Section 3.4. Thus we no longer use the derivatives of the conserved variables, but the discrete analogue in terms of their *jumps* across a cell interface:

$$\Delta\boldsymbol{U} = \begin{bmatrix}\Delta u_1\\ \Delta u_2\\ \Delta u_3\\ \Delta u_4\\ \Delta u_5\end{bmatrix} = \begin{bmatrix}\Delta m_{\mathrm{g}}\\ \Delta m_{\ell}\\ \Delta I_{\mathrm{g}}\\ \Delta I_{\ell}\\ \Delta E\end{bmatrix}. \tag{141}$$

The discrete variants of the differential rules for rational functions described in [18] allow us to rewrite the derivatives of the velocities (61)–(62) in terms of the jump Δ :

$$\Delta v_{\mathrm{g}} = \frac{\Delta u_3 - \overline{v}_{\mathrm{g}} \Delta u_1}{\overline{m}_{\mathrm{g}}}, \tag{142}$$

$$\Delta v_{\ell} = \frac{\Delta u_4 - \overline{v}_{\ell} \Delta u_2}{\overline{m}_{\ell}}, \tag{143}$$

where $\overline{(\cdot)}$ represents the arithmetic average.

The equations (63)–(65) can be rewritten as

$$\hat{a}_{3j} = \overline{I}_{\mathrm{g}} \frac{\Delta v_{\mathrm{g}}}{\Delta u_j} + \overline{v}_{\mathrm{g}} \frac{\Delta I_{\mathrm{g}}}{\Delta u_j} + \overline{\overline{\Delta_{\mathrm{i}} p}} \frac{\Delta \alpha_{\mathrm{g}}}{\Delta u_j} + \overline{\overline{\alpha_{\mathrm{g}}}} \frac{\Delta p}{\Delta u_j}, \tag{144}$$

$$\hat{a}_{4j} = \overline{I}_{\ell} \frac{\Delta v_{\ell}}{\Delta u_j} + \overline{v}_{\ell} \frac{\Delta I_{\ell}}{\Delta u_j} + \overline{\overline{\Delta_{\mathrm{i}} p}} \frac{\Delta \alpha_{\ell}}{\Delta u_j} + \overline{\overline{\alpha_{\ell}}} \frac{\Delta p}{\Delta u_j}, \tag{145}$$

$$\begin{aligned} \hat{a}_{5j} = {} & \overline{E}_{\mathrm{g}} \frac{\Delta v_{\mathrm{g}}}{\Delta u_j} + \overline{v}_{\mathrm{g}} \left\{ \overline{\left(e_{\mathrm{g}} + \frac{v_{\mathrm{g}}^2}{2} \right)} \frac{\Delta m_{\mathrm{g}}}{\Delta u_j} + \overline{m}_{\mathrm{g}} \left(\frac{\Delta e_{\mathrm{g}}}{\Delta u_j} + \overline{v}_{\mathrm{g}} \frac{\Delta v_{\mathrm{g}}}{\Delta u_j} \right) \right\} \\ & + \overline{E}_{\ell} \frac{\Delta v_{\ell}}{\Delta u_j} + \overline{v}_{\ell} \left\{ \overline{\left(e_{\ell} + \frac{v_{\ell}^2}{2} \right)} \frac{\Delta m_{\ell}}{\Delta u_j} + \overline{m}_{\ell} \left(\frac{\Delta e_{\ell}}{\Delta u_j} + \overline{v}_{\ell} \frac{\Delta v_{\ell}}{\Delta u_j} \right) \right\} \\ & + \overline{(\alpha_{\mathrm{g}} v_{\mathrm{g}} + \alpha_{\ell} v_{\ell})} \frac{\Delta p}{\Delta u_j} + \overline{p} \left\{ \overline{\alpha}_{\mathrm{g}} \frac{\Delta v_{\mathrm{g}}}{\Delta u_j} + \overline{\alpha}_{\ell} \frac{\Delta v_{\ell}}{\Delta u_j} + \overline{(v_{\mathrm{g}} - v_{\ell})} \frac{\Delta \alpha_{\mathrm{g}}}{\Delta u_j} \right\}. \end{aligned} \tag{146}$$

The two independent EOSes (68)–(69) will be given by

$$\Delta \rho_k = \hat{\mathfrak{a}}_k \Delta T + \hat{\mathfrak{b}}_k \Delta p, \tag{147}$$

$$\Delta e_k = \hat{\mathfrak{c}}_k \Delta T + \hat{\mathfrak{d}}_k \Delta \rho_k, \tag{148}$$

where $\hat{\mathfrak{a}}_k$, $\hat{\mathfrak{b}}_k$, $\hat{\mathfrak{c}}_k$ and $\hat{\mathfrak{d}}_k$ are the averages given by discrete variants of the differential product rule applied to rational functions.

The equation (71) may be written as

$$\frac{\Delta u_1}{\overline{\rho}_{\mathrm{g}}} + \frac{\Delta u_2}{\overline{\rho}_{\ell}} = \hat{q} \Delta T + \hat{r} \Delta p, \tag{149}$$

with

$$\hat{q} = \sum_k \frac{\overline{\alpha}_k \hat{\mathfrak{a}}_k}{\overline{\rho}_k}, \quad \hat{r} = \sum_k \frac{\overline{\alpha}_k \hat{\mathfrak{b}}_k}{\overline{\rho}_k}, \tag{150}$$

and finally, the equation for the total energy of the mixture (73) will by given by

$$\overline{m}_{\mathrm{g}} \Delta e_{\mathrm{g}} + \overline{m}_{\ell} \Delta e_{\ell} = \left(\overline{e}_{\mathrm{g}} - \frac{\hat{v}_{\mathrm{g}}^2}{2} \right) \Delta u_1 + \left(\overline{e}_{\ell} - \frac{\hat{v}_{\ell}^2}{2} \right) \Delta u_2 - \overline{v}_{\mathrm{g}} \Delta u_3 - \overline{v}_{\ell} \Delta u_4 + \Delta u_5, \tag{151}$$

where $\hat{v}_k^2/2 = \overline{v}_k^2 - \overline{v_k^2}/2$.

The results obtained by solving the system of equations given by (147)–(149) and (151) may be written as

$$\Delta p = \begin{bmatrix} \widehat{\partial p_1} \\ \widehat{\partial p_2} \\ \widehat{\partial p_3} \\ \widehat{\partial p_4} \\ \widehat{\partial p_5} \end{bmatrix}^T \Delta \boldsymbol{U} = \hat{\tau}^{-1} \begin{bmatrix} (\hat{v}_{\mathrm{g}}^2/2 - \overline{e}_{\mathrm{g}})\hat{q} - \sum_k \overline{m}_k \left(\hat{\mathfrak{a}}_k \hat{\mathfrak{d}}_k + \hat{\mathfrak{c}}_k\right)/\overline{\rho}_{\mathrm{g}} \\ (\hat{v}_{\ell}^2/2 - \overline{e}_{\ell})\hat{q} - \sum_k \overline{m}_k \left(\hat{\mathfrak{a}}_k \hat{\mathfrak{d}}_k + \hat{\mathfrak{c}}_k\right)/\overline{\rho}_{\ell} \\ -\overline{v}_{\mathrm{g}}\hat{q} \\ -\overline{v}_{\ell}\hat{q} \\ \hat{q} \end{bmatrix}^T \Delta \boldsymbol{U}, \tag{152}$$

$$\Delta e_{\mathrm{g}} = \begin{bmatrix} \widehat{\partial e_{\mathrm{g}_1}} \\ \widehat{\partial e_{\mathrm{g}_2}} \\ \widehat{\partial e_{\mathrm{g}_3}} \\ \widehat{\partial e_{\mathrm{g}_4}} \\ \widehat{\partial e_{\mathrm{g}_5}} \end{bmatrix}^T \Delta \boldsymbol{U} = \hat{\tau}^{-1} \begin{bmatrix} (\hat{v}_{\mathrm{g}}^2/2 - \overline{e}_{\mathrm{g}})\hat{z}_{\mathrm{g}} + \left(\hat{\mathfrak{d}}_{\mathrm{g}}\hat{\mu} + \overline{m}_{\ell}\hat{\xi}\right)/\overline{\rho}_{\mathrm{g}} \\ (\hat{v}_{\ell}^2/2 - \overline{e}_{\ell})\hat{z}_{\mathrm{g}} + \left(\hat{\mathfrak{d}}_{\mathrm{g}}\hat{\mu} + \overline{m}_{\ell}\hat{\xi}\right)/\overline{\rho}_{\ell} \\ -\overline{v}_{\mathrm{g}}\hat{z}_{\mathrm{g}} \\ -\overline{v}_{\ell}\hat{z}_{\mathrm{g}} \\ \hat{z}_{\mathrm{g}} \end{bmatrix}^T \Delta \boldsymbol{U}, \tag{153}$$

$$\Delta e_{\ell} = \begin{bmatrix} \widehat{\partial e_{\ell 1}} \\ \widehat{\partial e_{\ell 2}} \\ \widehat{\partial e_{\ell 3}} \\ \widehat{\partial e_{\ell 4}} \\ \widehat{\partial e_{\ell 5}} \end{bmatrix}^T \Delta \boldsymbol{U} = \hat{\tau}^{-1} \begin{bmatrix} (\hat{v}_{\mathrm{g}}^2/2 - \overline{e}_{\mathrm{g}})\hat{z}_{\ell} + \left(\hat{\mathfrak{d}}_{\ell}\hat{\eta} - \overline{m}_{\mathrm{g}}\hat{\xi}\right)/\overline{\rho}_{\mathrm{g}} \\ (\overline{v}_{\ell}^2/2 - \overline{e}_{\ell})\hat{z}_{\ell} + \left(\hat{\mathfrak{d}}_{\ell}\hat{\eta} - \overline{m}_{\mathrm{g}}\hat{\xi}\right)/\overline{\rho}_{\ell} \\ -\overline{v}_{\mathrm{g}}\hat{z}_{\ell} \\ -\overline{v}_{\ell}\hat{z}_{\ell} \\ \hat{z}_{\ell} \end{bmatrix}^T \Delta \boldsymbol{U}, \tag{154}$$

$$\Delta \rho_{\mathrm{g}} = \begin{bmatrix} \widehat{\partial \rho_{\mathrm{g}_1}} \\ \widehat{\partial \rho_{\mathrm{g}_2}} \\ \widehat{\partial \rho_{\mathrm{g}_3}} \\ \widehat{\partial \rho_{\mathrm{g}_4}} \\ \widehat{\partial \rho_{\mathrm{g}_5}} \end{bmatrix}^T \Delta \boldsymbol{U} = \hat{\tau}^{-1} \begin{bmatrix} (\hat{v}_{\mathrm{g}}^2/2 - \overline{e}_{\mathrm{g}})\hat{x}_{\mathrm{g}} + \left(\hat{\mu} - \hat{\mathfrak{b}}_{\mathrm{g}} \sum_k \overline{m}_k \hat{\mathfrak{c}}_k\right)/\overline{\rho}_{\mathrm{g}} \\ (\hat{v}_{\ell}^2/2 - \overline{e}_{\ell})\hat{x}_{\mathrm{g}} + \left(\hat{\mu} - \hat{\mathfrak{b}}_{\mathrm{g}} \sum_k \overline{m}_k \hat{\mathfrak{c}}_k\right)/\overline{\rho}_{\ell} \\ -\overline{v}_{\mathrm{g}}\hat{x}_{\mathrm{g}} \\ -\overline{v}_{\ell}\hat{x}_{\mathrm{g}} \\ \hat{x}_{\mathrm{g}} \end{bmatrix}^T \Delta \boldsymbol{U}, \tag{155}$$

where

$$\hat{\tau} = -\hat{r} \sum_k \overline{m}_k \left(\hat{\mathfrak{a}}_k \hat{\mathfrak{d}}_k + \hat{\mathfrak{c}}_k\right) + \hat{q} \sum_k \overline{m}_k \hat{\mathfrak{b}}_k \hat{\mathfrak{d}}_k, \tag{156}$$

$$\hat{x}_k = -\hat{\mathfrak{a}}_k \hat{r} + \hat{\mathfrak{b}}_k \hat{q}, \tag{157}$$

$$\hat{z}_k = -\hat{r}\left(\hat{\mathfrak{a}}_k \hat{\mathfrak{d}}_k + \hat{\mathfrak{c}}_k\right) + \hat{q}\hat{\mathfrak{b}}_k \hat{\mathfrak{d}}_k, \tag{158}$$

$$\hat{\xi} = \hat{\mathfrak{c}}_{\mathrm{g}} \hat{\mathfrak{b}}_{\ell} \hat{\mathfrak{d}}_{\ell} - \hat{\mathfrak{c}}_{\ell} \hat{\mathfrak{b}}_{\mathrm{g}} \hat{\mathfrak{d}}_{\mathrm{g}}, \tag{159}$$

$$\hat{\eta} = \overline{m}_{\mathrm{g}} \hat{\mathfrak{d}}_{\mathrm{g}} \left(\hat{\mathfrak{a}}_{\ell} \hat{\mathfrak{b}}_{\mathrm{g}} - \hat{\mathfrak{a}}_{\mathrm{g}} \hat{\mathfrak{b}}_{\ell}\right), \tag{160}$$

$$\hat{\mu} = \overline{m}_{\ell} \hat{\mathfrak{d}}_{\ell} \left(\hat{\mathfrak{a}}_{\mathrm{g}} \hat{\mathfrak{b}}_{\ell} - \hat{\mathfrak{a}}_{\ell} \hat{\mathfrak{b}}_{\mathrm{g}}\right). \tag{161}$$

The jumps in the gas volume fraction are given by

$$\Delta \alpha_{\mathrm{g}} = -\Delta \alpha_{\ell} = \frac{\Delta u_1}{\overline{\rho}_{\mathrm{g}}} - \frac{\overline{\alpha}_{\mathrm{g}}}{\overline{\rho}_{\mathrm{g}}} \Delta \rho_{\mathrm{g}}. \tag{162}$$

We are now in position to define the Roe matrix, which can be expressed in a similar way as the Jacobian matrix

$$\hat{\mathbf{A}} = \hat{\mathbf{A}}_c + \hat{\mathbf{A}}_{\alpha} + \hat{\mathbf{A}}_e + \hat{\mathbf{A}}_p, \tag{163}$$

where the convective matrix can be written as

$$\hat{\mathbf{A}}_c = \begin{bmatrix} 0 & 0 & 1 & 0 & 0 \\ 0 & 0 & 0 & 1 & 0 \\ -\overline{I}_{\rm g}\overline{v}_{\rm g}/\overline{m}_{\rm g} & 0 & \overline{I}_{\rm g}/\overline{m}_{\rm g} + \overline{v}_{\rm g} & 0 & 0 \\ 0 & -\overline{I}_\ell \overline{v}_\ell/\overline{m}_\ell & 0 & \overline{I}_\ell/\overline{m}_\ell + \overline{v}_\ell & 0 \\ \hat{a}_{c_1} & \hat{a}_{c_2} & \hat{a}_{c_3} & \hat{a}_{c_4} & 0 \end{bmatrix}, \tag{164}$$

with

$$\hat{a}_{c_1} = \overline{v}_{\rm g}\left(\overline{e}_{\rm g} - \frac{\hat{v}_{\rm g}^2}{2}\right) - \frac{\overline{E}_{\rm g}\overline{v}_{\rm g}}{\overline{m}_{\rm g}} - \overline{p}\left(\frac{\overline{\alpha}_{\rm g}\overline{v}_{\rm g}}{\overline{m}_{\rm g}} - \frac{\overline{(v_{\rm g} - v_\ell)}}{\overline{\rho}_{\rm g}}\right), \tag{165}$$

$$\hat{a}_{c_2} = \overline{v}_\ell\left(\overline{e}_\ell - \frac{\hat{v}_\ell^2}{2}\right) - \frac{\overline{E}_\ell\overline{v}_\ell}{\overline{m}_\ell} - \overline{p}\frac{\overline{\alpha}_\ell\overline{v}_\ell}{\overline{m}_\ell}, \tag{166}$$

$$\hat{a}_{c_3} = \overline{v}_{\rm g}^2 + \frac{\overline{E}_{\rm g}}{\overline{m}_{\rm g}} + \overline{p}\frac{\overline{\alpha}_{\rm g}}{\overline{m}_{\rm g}}, \tag{167}$$

$$\hat{a}_{c_4} = \overline{v}_\ell^2 + \frac{\overline{E}_\ell}{\overline{m}_\ell} + \overline{p}\frac{\overline{\alpha}_\ell}{\overline{m}_\ell}. \tag{168}$$

The volume-fraction matrix may be split as

$$\hat{\mathbf{A}}_\alpha = \frac{\overline{\overline{\Delta}_{\rm i} p\overline{\alpha}_{\rm g}}}{\overline{\rho}_{\rm g}}\hat{\mathbf{A}}_{\alpha_1} - \frac{\overline{p\overline{(v_{\rm g} - v_\ell)}\overline{\alpha_{\rm g}}}}{\overline{\rho_{\rm g}}}\hat{\mathbf{A}}_{\alpha_2} \tag{169}$$

with

$$\hat{\mathbf{A}}_{\alpha_1} = \begin{bmatrix} 0 & 0 & 0 & 0 & 0 \\ 0 & 0 & 0 & 0 & 0 \\ 1/\overline{\alpha}_{\rm g} - \widehat{\partial\rho_{\rm g}}_1 & -\widehat{\partial\rho_{\rm g}}_2 & -\widehat{\partial\rho_{\rm g}}_3 & -\widehat{\partial\rho_{\rm g}}_4 & -\widehat{\partial\rho_{\rm g}}_5 \\ \widehat{\partial\rho_{\rm g}}_1 - 1/\overline{\alpha}_{\rm g} & \widehat{\partial\rho_{\rm g}}_2 & \widehat{\partial\rho_{\rm g}}_3 & \widehat{\partial\rho_{\rm g}}_4 & \widehat{\partial\rho_{\rm g}}_5 \\ 0 & 0 & 0 & 0 & 0 \end{bmatrix}, \tag{170}$$

and

$$\hat{\mathbf{A}}_{\alpha_2} = \begin{bmatrix} 0 & 0 & 0 & 0 & 0 \\ 0 & 0 & 0 & 0 & 0 \\ 0 & 0 & 0 & 0 & 0 \\ 0 & 0 & 0 & 0 & 0 \\ \widehat{\partial\rho_{\rm g}}_1 - 1/\overline{\alpha}_{\rm g} & \widehat{\partial\rho_{\rm g}}_2 & \widehat{\partial\rho_{\rm g}}_3 & \widehat{\partial\rho_{\rm g}}_4 & \widehat{\partial\rho_{\rm g}}_5 \end{bmatrix}, \tag{171}$$

where we have used (155).

The energy matrix can be expressed as

$$\hat{\mathbf{A}}_c = \begin{bmatrix} 0 & 0 & 0 & 0 & 0 \\ 0 & 0 & 0 & 0 & 0 \\ 0 & 0 & 0 & 0 & 0 \\ 0 & 0 & 0 & 0 & 0 \\ \hat{a}_{e_1} & \hat{a}_{e_2} & -\overline{v}_{\rm g}\hat{a}_{e_5} & -\overline{v}_\ell\hat{a}_{e_5} & \hat{a}_{e_5} \end{bmatrix}, \tag{172}$$

with

$$\hat{a}_{e_1} = \sum_k \overline{m}_k \overline{v}_k \widehat{\partial e_{k1}}, \tag{173}$$

$$\hat{a}_{e_2} = \sum_k \overline{m}_k \overline{v}_k \widehat{\partial e_{k2}}, \tag{174}$$

$$\hat{a}_{e_5} = \sum_k \overline{m}_k \overline{v}_k \widehat{\partial e_{k5}}, \tag{175}$$

where we have used (153)–(154).

The pressure matrix may be written as

$$\hat{\mathbf{A}}_p = \begin{bmatrix} 0 & 0 & 0 & 0 & 0 \\ 0 & 0 & 0 & 0 & 0 \\ \overline{\overline{\alpha}}_{\mathrm{g}} \widehat{\partial p_1} & \overline{\overline{\alpha}}_{\mathrm{g}} \widehat{\partial p_2} & \overline{\overline{\alpha}}_{\mathrm{g}} \widehat{\partial p_3} & \overline{\overline{\alpha}}_{\mathrm{g}} \widehat{\partial p_4} & \overline{\overline{\alpha}}_{\mathrm{g}} \widehat{\partial p_5} \\ \overline{\overline{\alpha}}_{\ell} \widehat{\partial p_1} & \overline{\overline{\alpha}}_{\ell} \widehat{\partial p_2} & \overline{\overline{\alpha}}_{\ell} \widehat{\partial p_3} & \overline{\overline{\alpha}}_{\ell} \widehat{\partial p_4} & \overline{\overline{\alpha}}_{\ell} \widehat{\partial p_5} \\ \overline{v}_{\mathrm{m}} \widehat{\partial p_1} & \overline{v}_{\mathrm{m}} \widehat{\partial p_2} & \overline{v}_{\mathrm{m}} \widehat{\partial p_3} & \overline{v}_{\mathrm{m}} \widehat{\partial p_4} & \overline{v}_{\mathrm{m}} \widehat{\partial p_5} \end{bmatrix}, \tag{176}$$

where we have used (152).

This completes the description of the Roe matrix $\hat{\mathbf{A}}$. Our numerical algorithm is based on the wave-propagation (flux-difference splitting) form of Godunov's method presented by LeVeque [22, Chapter 15]. It has been employed for two-phase flow models e.g. in [18], and we omit details here for brevity.

6. Numerical Simulations

In the present section, we discuss the differences between the five-equation two-fluid model (TF_5) of Section 2.1 and the six-equation two-fluid model (TF_6) of Section 2.2 by performing numerical simulations.

The TF_5 model is solved numerically using the Roe scheme described in Section 5. A Roe scheme for the general TF_6 model is currently not available, and we have therefore employed the MUSCL-MUSTA6 scheme discussed in detail in [27]. Since we concentrate on the models themselves, we will in the following present results calculated on fine grids. Convergence tests and further discussion of the Roe scheme for TF_5 have been performed by Martínez [24].

All the calculations presented in the following were performed using a Courant–Friedrichs–Lewy (CFL) number of 0.5.

6.1. Thermodynamic State Relations

Following [1,7,30], among others, we assume that the fluids can be modelled using the stiffened-gas equation of state (EOS)

$$p = (\gamma_k - 1)\rho_k e_k - \gamma_k p_{\infty,k}, \tag{177}$$

where the ratio of specific heats, γ_k, and the 'reference' pressure, $p_{\infty,k}$, are constants for each phase. The temperature is found as

$$T_k = \frac{\gamma_k (e_k - p_{\infty,k}/\rho_k)}{c_{p,k}}. \tag{178}$$

For TF_6, the procedure for finding the primitive variables given the composite variables $\boldsymbol{U}$ involves solving a second-degree equation. Details can be found in [30]. For TF_5, we have employed the method by Flåtten *et al.* [16].

For the calculations presented in the following, we have made use of the equation-of-state parameters in Table 4, unless otherwise stated. These values have been used previously in [27, 30].

TABLE 4. Equation-of-state parameters for water and air.

	γ_k (–)	$p_{\infty,k}$ (Pa)	$c_{p,k}$ (J/(kg K))
gas (g)	1.4	0.0	1008.7
liquid (ℓ)	2.8	8.5×10^8	4186.0

TABLE 5. Initial state in Toumi's shock tube.

Quantity	Symbol (unit)	Left	Right
Gas vol. frac.	α_g (–)	0.25	0.10
Pressure	p (MPa)	20	10
Gas velocity	v_g (m/s)	0	0
Liquid velocity	v_ℓ (m/s)	0	0
Temperatures	$T_{\mathrm{g},\ell}$ (K)	308.15	308.15

TABLE 6. Initial state in the water-faucet test problem.

Quantity	Symbol (unit)	Value
Gas vol. frac.	α_g (–)	0.2
Pressure	p (MPa)	0.1
Gas velocity	v_g (m/s)	0.0
Liquid velocity	v_ℓ (m/s)	10.0
Temperatures	$T_{\mathrm{g},\ell}$ (K)	308.15

6.2. **Toumi's Shock Tube**

We start by considering Toumi's shock tube [41]. This problem has previously been studied e.g. in [14,30,38]. A tube of length 100 m is divided by a membrane in the middle. At $t = 0$, the membrane ruptures, and the flow starts evolving. The initial conditions are displayed in Table 5. For this problem, $\delta = 2$ has been utilized in the equation (27), as was also done in [14,30].

Figure 4 shows numerical results obtained for the time $t = 0.06$ s on a grid of 20000 cells. Here, the van Leer [44,45] slope was employed in the MUSCL-MUSTA6 scheme and the corresponding flux limiter was used in the Roe scheme. It can be observed that the five-equation (TF_5) and six-equation (TF_6) two-fluid models have solutions with differing wave speeds and plateau levels. For TF_6, only the liquid temperature has been plotted in Figure 4(d). Herein, the gas temperature deviates rather strongly from the common temperature of TF_5, due to the infinite temperature relaxation time of TF_6.

The differing wave speeds can also be illustrated by the plots in Figure 2 in Section 4.2, since the state of the water-air mixture under high pressure defined by Table 2 is the same as the initial state on the left-hand side of Toumi's shock tube. The numerical results in Figure 4 indicate that c_{TF_6} is roughly 15 % larger than c_{TF_5}. This is consistent with the relevant volume-fraction interval in Figure 2(b).

6.3. **Water Faucet**

The water-faucet test problem was introduced by Ransom [32] and has been been extensively studied in the literature, e.g. in [10,12,19,26,27,30,43].

The initial flow field is uniform, and the values are given in Table 6. The inlet boundary conditions are equal to the initial values for the gas volume fraction and for the gas and liquid velocities. A pressure equal to the initial pressure is specified at the outlet. At time $t = 0$, gravity ($g = 9.81\,\mathrm{m/s^2}$) starts working, and the liquid column begins to thin as a discontinuity moves towards the exit. In the following, the results are given at $t = 0.6$ s.

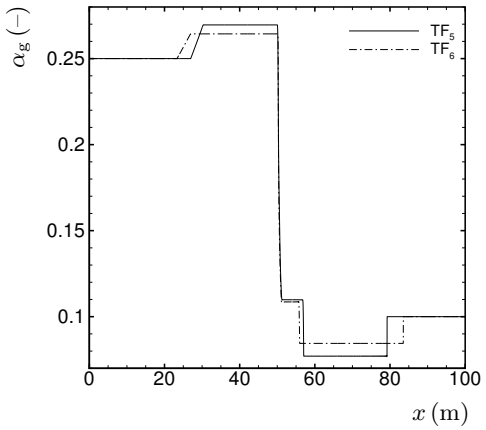

(a) Gas volume fraction.

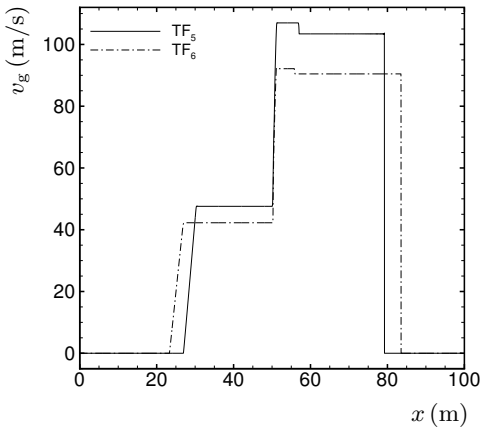

(b) Gas velocity.

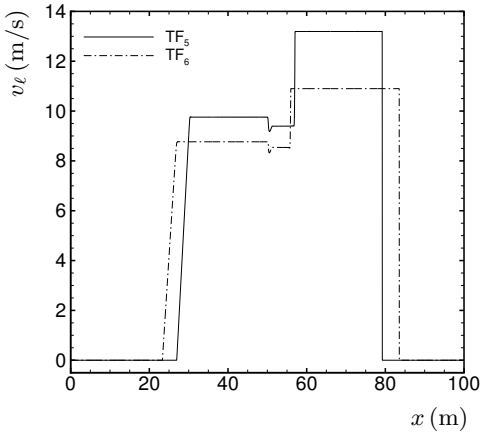

(c) Liquid velocity.

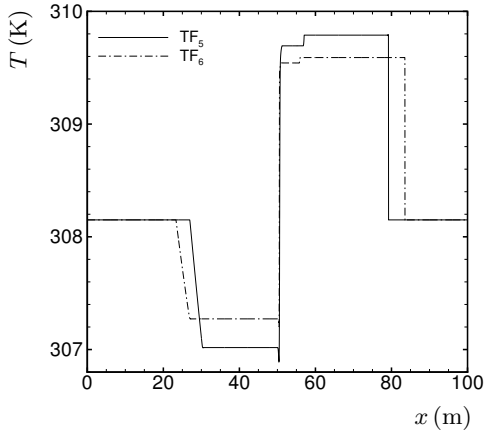

(d) Temperature (liquid phase).

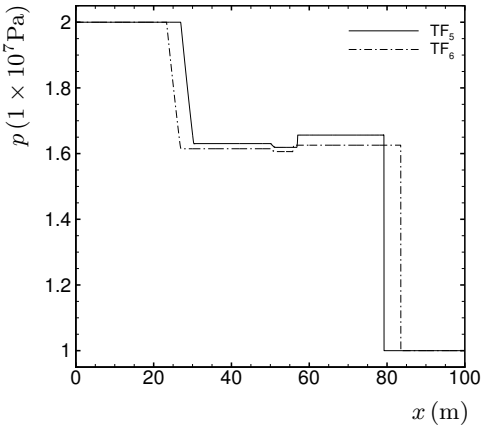

(e) Pressure.

FIGURE 4. Toumi's shock tube. Comparison between the five-equation (TF$_5$) and six-equation (TF$_6$) two-fluid models. High-resolution solutions on a 20000-cell grid.

TABLE 7. Equation-of-state parameters for CO_2.

	γ_k (–)	$p_{\infty,k}$ (Pa)	$c_{p,k}$ (J/(kg K))
gas (g)	1.1	5.5×10^5	1900
liquid (ℓ)	1.4	1.9×10^8	2500

TABLE 8. Initial state in the depressurization cases.

Quantity	Symbol (unit)	Water-air	CO_2
Gas vol. frac.	α_g (–)	0.2	0.2
Pressure	p (MPa)	10	5
Gas velocity	v_g (m/s)	0	0
Liquid velocity	v_ℓ (m/s)	0	0
Temperatures	$T_{g,\ell}$ (K)	300	273

Munkejord [26] found that the pressure in the water-faucet test problem is sensitive to the boundary conditions. Some remarks about the boundary conditions for TF$_6$ are given in [27].

Calculations were run on a grid of 10000 cells. The monotonized central-difference (MC) slope limiter [45] was employed in the MUSCL-MUSTA6 scheme and the corresponding flux limiter was used in the Roe scheme.

The physical variables are plotted in Figure 5. It can be seen that the temperature predicted by TF$_5$ is virtually identical to the liquid temperature in TF$_6$. The velocities and volume fractions are equal to plotting accuracy. The pressure plots, on the other hand, have different shapes. This is mainly due to the different pressure-propagation velocity (sound speed) in the two models. Different sound speeds will lead to the pressure waves reaching and being reflected at the boundaries at different times.

The state of the water-air mixture under atmospheric conditions defined by Table 1 in Section 4.1 is similar to the initial state of the present test problem. Figure 1(b) therefore illustrates that the root of the different pressure profiles in Figure 5(e) is the differing sound speed in TF$_5$ and TF$_6$.

6.4. **Pipe Depressurization**

The present test problem is constructed to have some resemblance to cases that may be of industrial interest, for instance in the field of CO_2 transport, where knowledge of the depressurization behaviour is of relevance for pipeline design, operations and integrity analysis.

A pipe of length 1000 m is closed at the left-hand side. Initially, the fluid is at rest. At $t = 0$, the pressure at the right-hand side is reduced, and a rarefaction wave propagates to the left. Two alternatives are considered, one with water-air and the EOS parameters of Table 4, and one with CO_2 and the EOS parameters of Table 7. Both are calculated on a 10000-cell grid employing the minmod limiter. The initial state for both cases is given in Table 8. For the water-air case, the imposed pressure at the left-hand side is 3 MPa, while it is 1 MPa for the CO_2 case.

Figure 6 shows the pressure for the water-air case. In Figure 6(a), the pressure is plotted along the pipe at the final time, while it is plotted as a function of time at one point in Figure 6(b). These graphs can be compared to the ones for the CO_2 case displayed in Figure 7. It can be seen that in both cases, TF$_6$ predicts a faster pressure propagation than TF$_5$, and that the difference is larger in the case of water-air. This can be understood by comparing the speeds of sound. In the water-air case, the maximum ratio $c_{\text{TF}_6}/c_{\text{TF}_5}$ is about 16 % (see Figure 2 for Toumi's shock tube which is very similar to the present case), while it is lower than 4 % for the CO_2 case of Figure 3. The main reason for this difference is that water and air have larger density and speed-of-sound ratios than CO_2 liquid and gas, see (134).

This test illustrates that in cases where the pressure and its propagation is of interest, the modelling assumptions regarding interphasic heat transfer may significantly influence the results. This holds even if the system

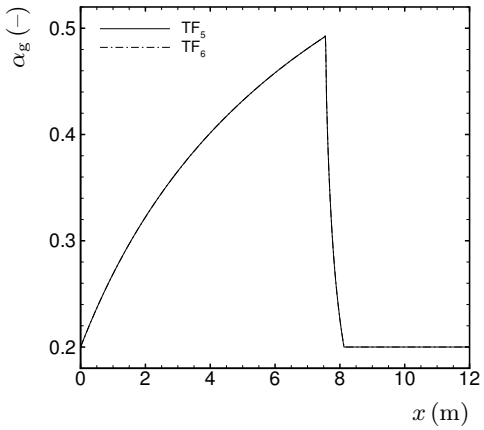

(a) Gas volume fraction.

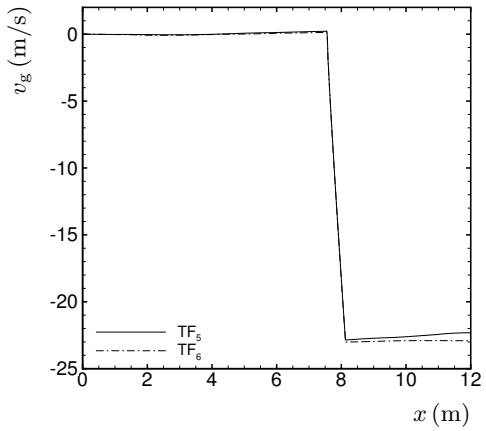

(b) Gas velocity.

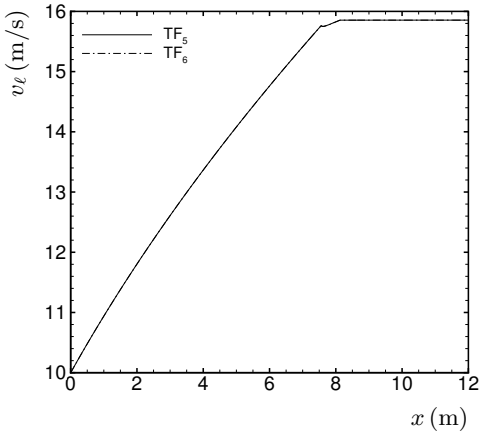

(c) Liquid velocity.

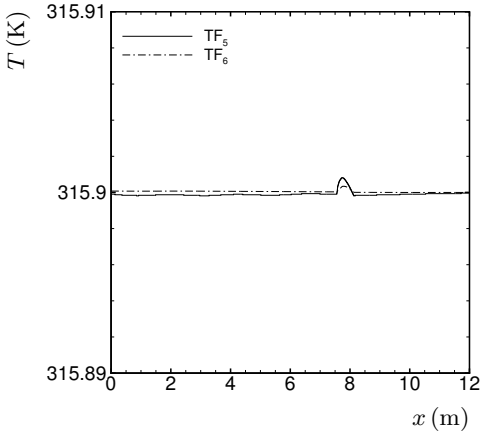

(d) Temperature (liquid phase).

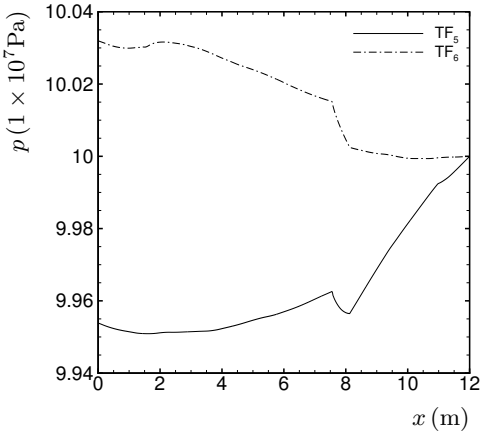

(e) Pressure.

FIGURE 5. Water-faucet problem. Comparison between the five-equation (TF$_5$) and six-equation (TF$_6$) two-fluid models. High-resolution solutions on a 10000-cell grid.

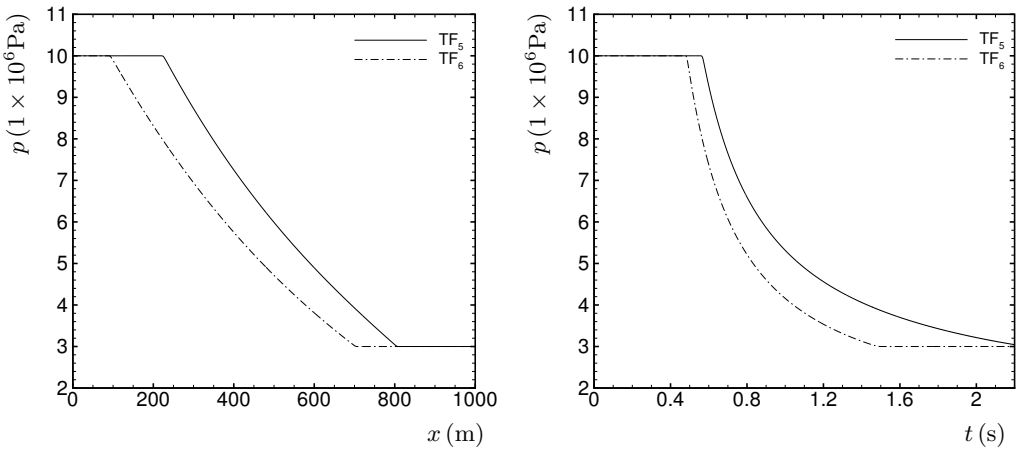

(a) $t = 2.2\,\mathrm{s}$. (b) $x = 800\,\mathrm{m}$.

FIGURE 6. Pressure for the water-air pipe depressurization. Comparison between the five-equation (TF$_5$) and six-equation (TF$_6$) two-fluid models. High-resolution solutions on a 10000-cell grid.

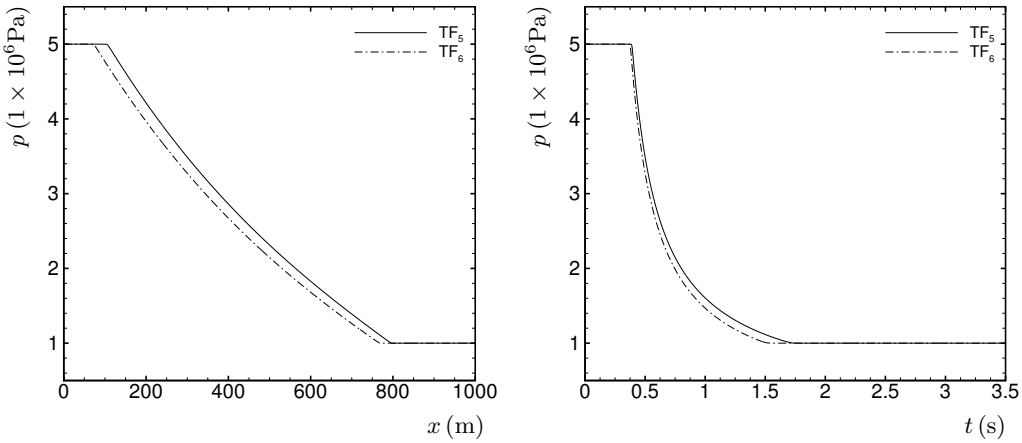

(a) $t = 3.5\,\mathrm{s}$. (b) $x = 900\,\mathrm{m}$.

FIGURE 7. Pressure for the CO_2 pipe depressurization. Comparison between the five-equation (TF$_5$) and six-equation (TF$_6$) two-fluid models. High-resolution solutions on a 10000-cell grid.

remains close to thermal equilibrium. The main purpose of this section has been to investigate this effect in the transition from the TF$_6$ to the TF$_5$ model.

In this respect, our focus has been to shed some light on the *mathematical* properties of these models. We do, however, wish to remark that for real-world phenomena, velocity relaxation may take place on a time scale short enough to significantly impact the pressure waves. This means that both the TF$_6$ and the TF$_5$ models could predict a too rapid propagation of these waves. We refer to [46] and references therein for a further discussion.

7. Summary

We have studied a thermally relaxed two-fluid model, with an emphasis on understanding how the relaxation procedure influences the propagation velocity of pressure waves. A main result has been a proof that the temperature-relaxation procedure satisfies a subcharacteristic condition. In this respect, we have also derived the results (118)–(119), which simply and perhaps surprisingly relate the effects of temperature and velocity relaxation in two-phase pipe flow models. A main conclusion of this work is stated in Section 4.3.1, where we argue that the effect of thermal relaxation is largest for mixtures that have a large difference in density and sound velocity between the two phases, as given by the ratio (135).

These results have been verified by numerical simulations, performed by the aid of a Roe-type scheme augmented with a high-resolution wave limiter.

Acknowledgements

This work was financed through the CO_2 Dynamics project. The authors acknowledge the support from the Research Council of Norway (189978), Gassco AS, Statoil Petroleum AS and Vattenfall AB.

We thank the editor and the anonymous reviewers for their kind remarks which led to improvements on the first version of this paper.

References

[1] R. Abgrall and R. Saurel, Discrete equations for physical and numerical compressible multiphase mixtures, *J. Comput. Phys.* **186**, 361–396, (2003).
[2] M. R. Baer and J. W. Nunziato, A two-phase mixture theory for the deflagration-to-detonation transition (DDT) in reactive granular materials, *Int. J. Multiphase Flow* **12**, 861–889 (1986).
[3] M. Baudin, C. Berthon, F. Coquel, R. Masson and Q. H. Tran, A relaxation method for two-phase flow models with hydrodynamic closure law, *Numer. Math.* **99**, 411–440, (2005).
[4] M. Baudin, F. Coquel and Q. H. Tran, A semi-implicit relaxation scheme for modeling two-phase flow in a pipeline, *SIAM J. Sci. Comput.* **27**, 914–936 (2005).
[5] K. H. Bendiksen, D. Malnes, R. Moe, and S. Nuland, The dynamic two-fluid model OLGA: Theory and application, in *SPE Prod. Eng.* **6**, 171–180, (1991).
[6] D. Bestion, The physical closure laws in the CATHARE code, *Nucl. Eng. Des.* **124**, 229–245, (1990).
[7] C.-H. Chang and M.-S. Liou, A robust and accurate approach to computing compressible multiphase flow: Stratified flow model and AUSM$^+$-up scheme, *J. Comput. Phys.* **225**, 850–873, (2007).
[8] G.-Q. Chen, C. D. Levermore and T.-P. Liu, Hyperbolic conservation laws with stiff relaxation terms and entropy, *Comm. Pure Appl. Math.* **47**, 787–830, (1994).
[9] P. Cinnella, Roe-type schemes for dense gas flow computations, *Comput. Fluids* **35** 1264–1281, (2006).
[10] F. Coquel, K. El Amine, E. Godlewski, B. Perthame and P. Rascle, A numerical method using upwind schemes for the resolution of two-phase flows, *J. Comput. Phys.* **136**, 272–288, (1997).
[11] F. Coquel, Q. L. Nguyen, M. Postel and Q. H. Tran, Entropy-satisfying relaxation method with large time-steps for Euler IBVPs, *Math. Comput.* **79**, 1493–1533, (2010).
[12] S. Evje and T. Flåtten, Hybrid flux-splitting schemes for a common two-fluid model, *J. Comput. Phys.* **192**, 175–210, (2003).
[13] S. Evje and K. K. Fjelde, Relaxation schemes for the calculation of two-phase flow in pipes, *Math. Comput. Modelling* **36**, 535–567, (2002).
[14] S. Evje and T. Flåtten, Hybrid central-upwind schemes for numerical resolution of two-phase flows, *ESAIM – Math. Model. Num.* **39**, 253–273, (2005).
[15] S. Evje and T. Flåtten, On the wave structure of two-phase flow models, *SIAM J. Appl. Math.* **67**, 487–511, (2007).
[16] T. Flåtten, A. Morin and S. T. Munkejord, On solutions to equilibrium problems for systems of stiffened gases, *SIAM J. Appl. Math.*, **71**, 41–67, (2011).
[17] T. Flåtten, A. Morin and S. T. Munkejord, Wave propagation in multicomponent flow models, *SIAM J. Appl. Math.*, **70**, 2861–2882, (2010).
[18] T. Flåtten and S.T. Munkejord, The approximate Riemann solver of Roe applied to a drift-flux two-phase flow model, *ESAIM – Math. Model. Num.* **40**, 735–764, (2006).
[19] H. Guillard and F. Duval, A Darcy law for the drift velocity in a two-phase flow model, *J. Comput. Phys.* **224**, 288–313 (2007).
[20] S. Jin and Z. Xin, The relaxation schemes for systems of conservation laws in arbitrary space dimensions, *Comm. Pure Appl. Math.* **48**, 235–276, (1995).

[21] K. H. Karlsen, C. Klingenberg and N. H. Risebro, A relaxation scheme for conservation laws with a discontinuous coefficient, *Math. Comput.* **73**, 1235–1259, (2004).
[22] R. J. LeVeque, *Finite Volume Methods for Hyperbolic Problems*, Cambridge University Press, Cambridge, UK (2002).
[23] T.-P. Liu, Hyperbolic conservation laws with relaxation, *Commun. Math. Phys.* **108**, 153–175, (1987).
[24] P. J. Martínez Ferrer, *Numerical and mathematical analysis of a five-equation model for two-phase flow*, Master's thesis, SINTEF Energy Research, Trondheim, Norway, October 2010. Available from `http://www.sintef.no/Projectweb/CO2-Dynamics/Publications/`.
[25] J. M. Masella, Q. H. Tran, D. Ferre and C. Pauchon, Transient simulation of two-phase flows in pipes, *Int. J. Multiphase Flow* **24**, 739–755, (1998).
[26] S. T. Munkejord, Partially-reflecting boundary conditions for transient two-phase flow, *Commun. Numer. Meth. En.* **22**, 781–795, (2007).
[27] S. T. Munkejord, S. Evje and T. Flåtten, A MUSTA scheme for a nonconservative two-fluid model, *SIAM J. Sci. Comput.* **31**, 2587–2622, (2009).
[28] A. Murrone and H. Guillard, A five equation reduced model for compressible two phase flow problems, *J. Comput. Phys.* **202**, 664–698, (2005).
[29] R. Natalini, Recent results on hyperbolic relaxation problems. Analysis of systems of conservation laws, in *Chapman & Hall/CRC Monogr. Surv. Pure Appl. Math.*, 99, Chapman & Hall/CRC, Boca Raton, FL, 128–198, (1999).
[30] H. Paillère, C. Corre and J. R. Carcía Gascales, On the extension of the AUSM+ scheme to compressible two-fluid models, *Comput. Fluids* **32**, 891–916, (2003).
[31] L. Pareschi and G. Russo, Implicit-explicit Runge-Kutta schemes and applications to hyperbolic systems with relaxation, *J. Sci. Comput.* **25**, 129–155, (2005).
[32] V. H. Ransom, Faucet Flow, In: G. F. Hewitt, J. M. Delhaye and N. Zuber, editors, *Numerical Benchmark Tests*, volume 3 of *Multiphase Science and Technology*, pp. 465–467. Hemisphere/Springer, Washington, USA, (1987).
[33] P. L. Roe, Approximate Riemann solvers, parameter vectors, and difference schemes, *J. Comput. Phys.* **43**, 357–372 (1981).
[34] R. Saurel and R. Abgrall, A multiphase Godunov method for compressible multifluid and multiphase flows, *J. Comput. Phys.* **150**, 425–467, (1999).
[35] R. Saurel, F. Petitpas and R. Abgrall, Modelling phase transition in metastable liquids: application to cavitating and flashing flows, *J. Fluid Mech.* **607**, 313–350, (2008).
[36] H. B. Stewart and B. Wendroff, Two-phase flow: Models and methods, *J. Comput. Phys.* **56**, 363–409, (1984).
[37] J. H. Stuhmiller, The influence of interfacial pressure forces on the character of two-phase flow model equations, *Int. J. Multiphase Flow* **3**, 551–560, (1977).
[38] I. Tiselj and S. Petelin, Modelling of two-phase flow with second-order accurate scheme, *J. Comput. Phys.* **136**, 503–521, (1997).
[39] WAHA3 Code Manual, *JSI Report IJS-DP-8841*, Jožef Stefan Institute, Ljubljana, Slovenia, (2004).
[40] I. Toumi, A weak formulation of Roe's approximate Riemann solver, *J. Comput. Phys.* **102**, 360–373, (1992).
[41] I. Toumi, An upwind numerical method for two-fluid two-phase flow models, *Nucl. Sci. Eng.* **123**, 147–168, (1996).
[42] Q. H. Tran, M. Baudin and F. Coquel, A relaxation method via the Born-Infeld system, *Math. Mod. Meth. Appl. S.* **19**, 1203–1240, (2009).
[43] J. A. Trapp and R. A. Riemke, A nearly-implicit hydrodynamic numerical scheme for two-phase flows, *J. Comput. Phys.* **66**, 62–82, (1986).
[44] B. van Leer, Towards the ultimate conservative difference scheme II. Monotonicity and conservation combined in a second-order scheme, *J. Comput. Phys.* **14** 361–370, (1974).
[45] B. van Leer, Towards the ultimate conservative difference scheme IV. A new approach to numerical convection, *J. Comput. Phys.* **23**, 276–299, (1977).
[46] A. Zein, M. Hantke and G. Warnecke, Modeling phase transition for compressible two-phase flows applied to metastable liquids, *J. Comput. Phys.* **229**, 2964–2998, (2010).
[47] N. Zuber and J. A. Findlay, Average volumetric concentration in two-phase flow systems, *J. Heat Transfer* **87**, 453–468, (1965).